North American Journal of Fisheries Management 42:1111–1133, 2022

ISSN: 0275-5947 print / 1548-8675 online
DOI: 10.1002/nafm.10799

ARTICLE

Understanding Salmon Migration Dynamics in a Data-Limited Environment

Rebecca A. Buchanan* and Steven L. Whitlock
Columbia Basin Research, School of Aquatic and Fishery Sciences, University of Washington, 1325 4th Avenue, Suite 1515, Seattle, Washington 98101-2540, USA

Abstract
Effective management of natural resources and migratory fish populations depends on understanding the relationship between life cycle parameters, management decisions, and environmental conditions. However, the difficulty of data collection can result in small or nonrepresentative data sets, thus limiting the accuracy and utility of modeling results. This is especially true for studies of migratory species in changing environments. In such situations, reevaluating previous results in light of new data is an essential exercise. We used three additional years of acoustic telemetry data to assess and update previous statistical models of survival of juvenile fall-run Chinook Salmon *Oncorhynchus tshawytscha* smolts emigrating through the southern portion of the Sacramento–San Joaquin River Delta (hereafter, "Delta") in California. Some previously identified relationships were maintained with the additional data, including the significance of water flow measures in areas outside the main-stem migration route and the role of water temperature and river discharge into the system for upstream reaches. The net downstream-directed discharge in the interior Delta was associated with fish movement to a large water pumping facility, but its perceived importance in the original analysis depended on a single dominant study year. Survival in dry years was predicted to be higher in the upstream region of the main-stem San Joaquin River when a temporary rock barrier limited entry of fish and river flow to the first distributary encountered in the Delta. In normal and wet years, through-Delta survival was predicted to be higher for fish that departed the main-stem river at that distributary. However, considerable uncertainty remains in the modeling results. Additional monitoring will be necessary to further reduce uncertainty and ensure that the modeling results reflect the system as it responds to climate change.

Centuries of intense resource use and land use changes have negatively affected anadromous fish populations (Nehlsen et al. 1991; Duncan and Lockwood 2001; Reynolds et al. 2005), and these effects are likely to be exacerbated by climate change (Poff et al. 2002). Increasing demand for finite water resources has required management of systems to meet multiple objectives in order to sustain native, iconic, or economically important fishery resources as well as the human populations living nearby (Kehoe et al. 2021). Science-based management begins with the development of conceptual models of how decisions and ecosystem processes affect fish and wildlife population dynamics, followed by quantitative models that are used to assess assumptions, weigh competing hypotheses, and make predictions (Walters 1986; Conroy and Peterson 2013). However, data on stressed populations are often scarce and establishing relationships between survival and potential drivers can be challenging. Data sets involving short time series are especially problematic because available observations may fail to represent the full range of variability in either environmental and management conditions or population response. Consequently, models based on short time series may generate unexpected statistical relationships and result in inappropriate management decisions (Wenger and Olden 2012). Given the combination of limited data and a highly variable

*Corresponding author: rabuchan@uw.edu
Received February 1, 2022; accepted May 26, 2022

environment, it may be unclear in such situations whether the estimated relationships truly represent a shift in ecosystem processes or are merely an artifact of sampling variability. In these situations, new data from additional years of study are invaluable to both test and update existing models.

Chinook Salmon *Oncorhynchus tshawytscha* from the Central Valley of California represent a case in point. Fall-run Chinook Salmon from this region have been classified as a species of special concern by the National Marine Fisheries Service and the California Department of Fish and Wildlife (Moyle et al. 2017). The population has declined following a combination of overharvest, hatchery impacts, and the introduction of nonnative species, as well as habitat degradation and loss resulting from mining, dam construction, water diversions, drought, and climate change (Fisher 1994; Yoshiyama et al. 1998; Moyle et al. 2017; Sabal et al. 2019). This population is near the southern tip of the species' indigenous range and forms the basis of the California–southern Oregon ocean salmon fishery, as well as serving as an important prey base for endangered killer whales *Orcinus orca* (NMFS 2009). The San Joaquin River (SJR) basin component of the population has had particularly low survival during juvenile emigration (Buchanan et al. 2018), and resource managers are faced with identifying conditions and management actions that are conducive to higher emigration survival.

Of particular interest is survival during juvenile emigration through the Sacramento–SJR Delta (hereafter, "Delta"), the upstream region of a tidally influenced river estuary (Figure 1). The Delta is a hydrologically complex region with numerous natural and artificial channels and is home to two large water pumping facilities that extract water from the Delta and export it elsewhere in the state for municipal and agricultural use (Grimaldo et al. 2011). Hydrodynamic conditions in the Delta are influenced by tides, releases of water from upstream reservoirs, manipulation of the water pumping operations, and use of barriers intended to limit flow of water or fish into certain regions (NMFS 2009). Fish in the interior Delta (i.e., west and south of the SJR; Figure 1) are at risk of entrainment in the water pumping facilities, where they may be lost to the pumps or conveyance canals, delayed by increased pumping rates, or subject to predation by the large population of predator fishes in or near the entrances to the facilities (Gingras 1997; Kimmerer 2008; NMFS 2009).

Salmon and water management in the Delta has been based partly on a conceptual model (Table 1) that predicts higher through-Delta survival when (1) higher river discharge enters the Delta ("Delta inflow"), (2) flow in the interior Delta is directed away from the facilities (i.e., north toward the Pacific Ocean), (3) water pumping rates ("export rates" or simply "exports") are lower, (4) fish use the main-stem river route through the Delta (i.e., avoid the interior Delta), and (5) entry to the primary interior Delta route is blocked with a temporary manmade barrier (NMFS 2009). The conceptual model is based partly on an understanding of the physiological needs of migrating salmon (e.g., water quality considerations; Lehman et al. 2017) and the potential for mortality at the water pumping facilities (e.g., Gingras 1997) and partly on conceptions of regional differences in both mortality risk and hydrodynamic response to management actions involving inflow, exports, and installation of temporary instream barriers. Briefly, the expectation is that more freshwater directed downstream is better, as is avoidance of the interior Delta and the water pumping facilities (Kimmerer 2002, 2008; Newman 2003; Newman and Brandes 2010; Perry et al. 2010; Michel et al. 2015). Points 1–4 above are assumed to hold for fish emigrating from either the SJR or the Sacramento River (SR). Point 5 is assumed to hold for SJR stocks, referring to a rock barrier that is sometimes installed in the spring to limit fish entry into the SJR's primary distributary (Old River [OR]), which leads past the entrance to the water pumping facilities. Management of river flows in the Delta is costly, requiring releases of water from upstream reservoirs and restrictions of export rates. Thus, natural resource agency managers are interested in knowing how well the actual salmon emigration dynamics agree with the conceptual model.

A multiyear telemetry study was conducted in 2007–2017 to estimate survival of juvenile fall-run Chinook Salmon during their emigration from the lower SJR through the Delta. The first few study years acted as pilot studies while study design, field methods, and tag technology were tested. A standardized set of protocols and study designs was used starting in 2010, and a multiyear analysis of large- and intermediate-scale survival was performed using study years 2010–2014 to address managers' questions regarding the conceptual model predictions (Buchanan and Skalski 2020). The results showed a surprising lack of consistency with several facets of the conceptual model. Although survival through the upstream part of the Delta was found to be positively associated with Delta inflow and was higher when the temporary barrier was installed, no strong association was observed between total survival through the Delta and Delta inflow, export rate, primary migration route, or barrier presence. Instead, total survival was positively associated with the volume—but not the direction—of water flow measured in the interior Delta. It was unclear whether the lack of support for the a priori assumptions reflected a true failing of the conceptual model for this population or whether it resulted from using data from a small number of study years in a system that can exhibit a high degree of heterogeneity in conditions. In particular, only one study year represented wet hydrologic conditions, while three other years represented drought conditions. Additionally, the survival probability

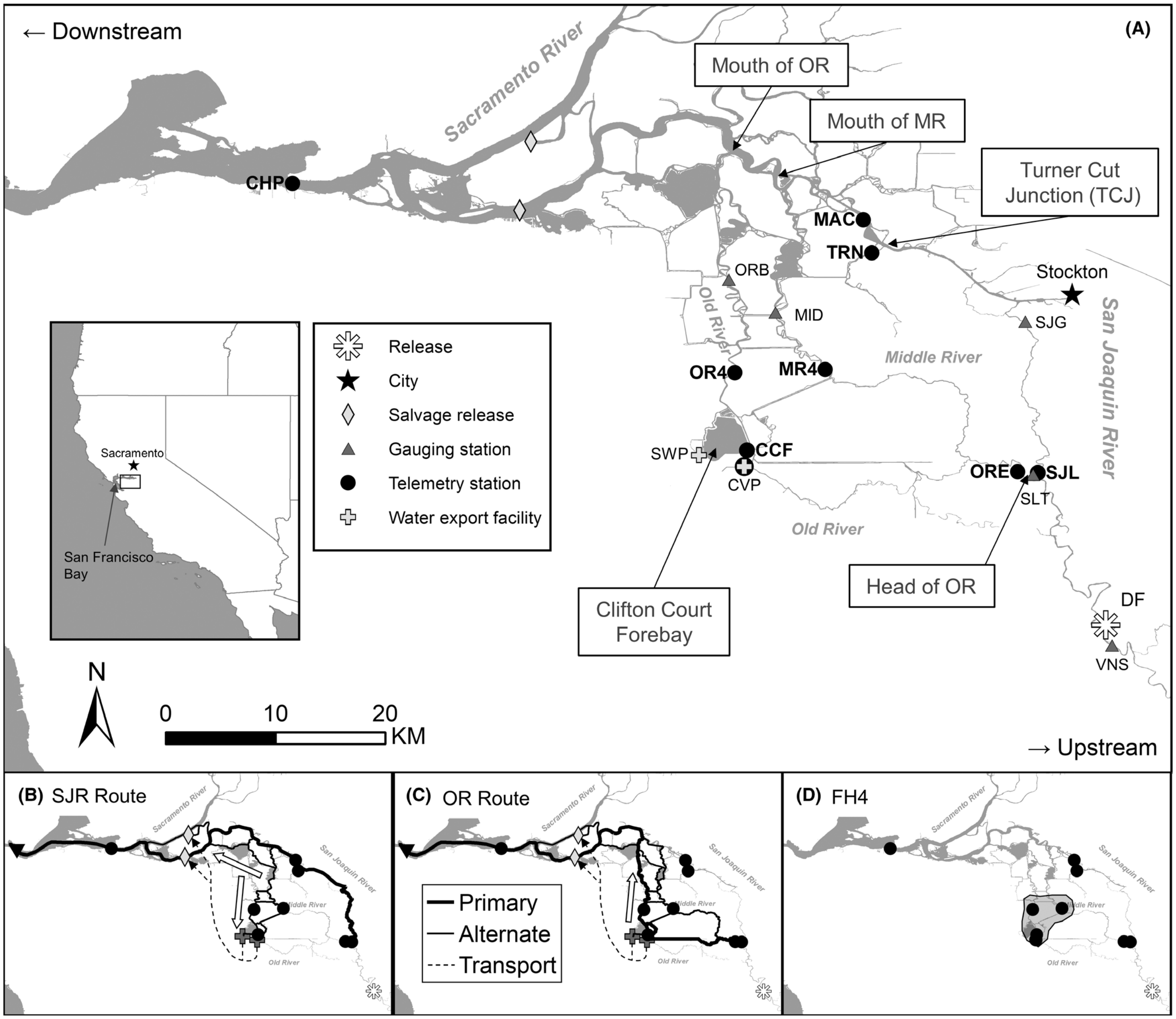

FIGURE 1. **(A)** The study area in the southern Sacramento–San Joaquin River Delta and major routes through the study area: **(B)** San Joaquin River (SJR) route, **(C)** Old River (OR) route from the head of OR to Chipps Island, and **(D)** the FH4 region, encompassing detection at the water export facilities and Highway 4 stations (shaded region). White arrows on route maps indicate the predominant direction of fish movement through the interior Delta. Marked locations are the Durham Ferry (DF) release site, key cities, acoustic telemetry stations, river gauging stations, and salvage facilities. Inset map (in panel a) shows the state of California, United States (light shading), and the Delta, San Francisco Bay, and Pacific Ocean (dark shading); detailed area is marked with a rectangle. Water export and salvage facilities are the Central Valley Project (CVP) and State Water Project (SWP). Telemetry and gauging station codes are defined in Table 3.

was modeled separately for each year (fixed year effects). This approach accommodated heterogeneity in fish and habitat conditions unrelated to the covariates considered, and it aided in uncovering associations between covariates and survival; however, it also limited use of the model to predict survival in future years. Furthermore, that analysis did not explicitly model survival in the critical region between Delta entry and the water pumping facilities.

Since the original model was developed, the telemetry study was extended two additional years (2016, 2017), including one very wet year (2017). Furthermore, observation data from one of the early years (2009) were reprocessed using methods from subsequent years. Collectively, these three additional years of data provide an opportunity to (1) test whether the understanding arising from the 2010–2014 models reflects survival patterns in other years

TABLE 1. Conceptual model of anticipated effects of operational factors on the survival of emigrating salmon smolts through the Sacramento–San Joaquin River Delta.

Operational factor	Condition expected for higher survival	Hypothesized mortality mechanisms
1. Delta inflow	Higher inflow	Entrainment,[a] thermal stress,[b] disease,[c] contaminant stress,[c,d] and predation[e]
2. Net flow direction in the interior Delta	Net positive flow toward the Pacific Ocean	Entrainment[a] and predation[e]
3. Water exports	Lower exports	Entrainment[a] and predation[e]
4. Routing through the Delta	Main-stem river route	Entrainment,[a] contaminant stress,[d] and predation[e]
5. Barriers to interior Delta entry	Barrier installation at the head of Old River (diverts fish and flow into the main-stem route)	Entrainment,[a] thermal stress,[b] contaminant stress,[d] and predation[e]

[a]Kimmerer (2008).
[b]Lehman et al. (2017).
[c]Lehman et al. (2020).
[d]Moyle et al. (2017).
[e]Michel et al. (2018).

and (2) extend that analysis using a more representative data set. Although they are not true replicates in a rigorous experimental design sense (Hurlbert 1984), data from the high-water year of 2017 and even the "below-normal" water year (WY) of 2009 provide needed pseudoreplicates of these poorly represented conditions. In addition to assessing and updating the original model, the expanded data set provides an opportunity to investigate hypotheses relating to potential interactions between management actions or migration strategies and environmental conditions. For instance, it has been hypothesized that the benefit of the rock barrier results from increased river flow directed down the main-stem SJR (i.e., prevented from entering OR) when the barrier is installed (Buchanan et al. 2021). If so, then the effect of increased Delta inflow on survival should be higher when the barrier is in place. Similarly, conditions in the interior Delta are hypothesized to have stronger effects on salmon in the OR route, which leads directly to the interior Delta, than in the SJR route (Cavallo et al. 2015). A related question involves identifying the optimal migration routing through the Delta under different conditions.

In this paper, we carry forward the work of determining reasonable models for characterizing the survival of Chinook Salmon as they migrate through the Delta. Our specific objectives are to (1) independently assess the quality of the predictions from the 2010–2014 model (Buchanan and Skalski 2020) for the new study years (2009, 2016, and 2017) and (2) update the 2010–2014 model using the full set of data (2009–2014, 2016–2017). In addition, we take the opportunity to explore the dependence of the original modeling results on a single study year, 2011, which was the only wet year in the original study and provided over half (52%) of the records available for the 2010–2014 study. We also add a new spatial element to the model, targeting survival to the critical region near two large water pumping facilities. Finally, we use the modeling results to investigate the differences in total survival in the two primary migration routes through the Delta and examine how the impact of route selection may vary with hydrological and environmental conditions.

METHODS

Study Area

The Delta is the upstream region of an inland, inverted tidal estuary where the SR and SJR converge with a series of bays that end in the San Francisco Bay and the Pacific Ocean (Figure 1). The SJR enters the Delta from the south, and the SR enters from the north; their confluence is at the Delta exit at Chipps Island, approximately 77 river kilometers (rkm) from the Golden Gate Bridge. The water in the Delta is primarily freshwater, and the western region is seasonally brackish, with freshwater inputs from the rivers and saltwater inputs from the bays via tidal action. Delta inflow is largely controlled by releases from upstream reservoirs in all years except wet years, and the annual hydrograph has shifted from high spring inflows to increased inflows in the late summer and fall when water is needed for agriculture (Arthur et al. 1996; Kimmerer 2002).

This study focused on the southern portion of the Delta, which is bounded on the east and north by the SJR (Figure 1). The southern Delta entry is near Mossdale Bridge (Mossdale; 174 rkm from the Golden Gate Bridge). Two large water pumping facilities are located in the southwestern corner of the Delta off OR, which departs from the SJR near Lathrop, California, and rejoins it approximately 40 rkm upstream of Chipps Island. The pumping facilities are the C.W. Bill Jones Pumping Plant, part of the federal Central Valley Project (CVP), and the Harvey O. Banks Pumping Plant, part of the State Water Project (SWP). Both projects include fish facilities that collect ("salvage") a portion of the fish entering the projects; collection numbers increase with pumping rates (Kimmerer 2008; C. Karp, B. Wu, and A. Scultz, unpublished paper presented at the 48th annual meeting of the American Fisheries Society, 2014). Water extracted at these facilities is exported out of the Delta for municipal and agricultural use throughout the state.

The predominant flow of both water and salmon from the SJR basin was through OR historically (Erkkila et al. 1950). The temporary rock barrier sometimes installed at the source ("head") of OR thus blocks most of the flow from the historical route and diverts both water and salmon into the main-stem SJR along the eastern boundary of the Delta. Without the barrier, the majority of the SJR water entering the Delta is exported at the CVP (Arthur et al. 1996; Kimmerer and Nobriga 2008). During periods of low Delta inflow and high export rates, the SR provides most of the freshwater in the interior Delta, with the predominant pattern of water movement from the SR southward to the water export facilities (Arthur et al. 1996; Monsen et al. 2007). Protective measures are in place to limit water export operations in the spring when salmon and steelhead *O. mykiss* (anadromous Rainbow Trout) are migrating (NMFS 2009). The dual forces of tides and water pumping can result in reverse flows in OR and the Middle River (MR) north of the pumping plants; depending on the tidal cycle and export operations, river flow in this region may be directed either north toward the bays and ocean ("positive flow") or south toward the pumping facilities ("negative flow"). In addition to complex hydrodynamics, the interior Delta is characterized by several submerged agricultural tracts that are effectively tidal lakes hosting a large community of nonnative submerged aquatic vegetation and fishes, including predators such as Largemouth Bass *Micropterus salmoides* (Young et al. 2018).

Salmon entering the southern Delta from the SJR may either (1) remain in the SJR at the head of OR (HOR) or (2) enter OR (Figure 1). Those that remain in the SJR at that junction either may migrate to the Delta exit without leaving the main-stem river or may leave the SJR at any of several points downstream to enter the interior Delta. The first entry point after the HOR is Turner Cut, located northwest of Stockton, California. Fish that enter OR at its head may make their way to the Delta exit entirely in the OR, or they may subsequently enter MR, the source of which is approximately 7 rkm west of the HOR. Alternatively, they may enter the water export facilities. Some fish that are entrained in these facilities are directed by louvers into holding tanks (salvage), transported by truck around the rest of the Delta, and released back into the river approximately 20 rkm upstream of Chipps Island (Figure 1; Kimmerer 2008). Entrained fish that escape salvage are lost to the water conveyance canals or subject to predation within the facility and are treated as mortalities. In 3 years of this study, a temporary rock barrier was installed by the California Department of Water Resources (CDWR) at the HOR to limit access to OR from the SJR during the salmon emigration. Culverts in the barrier allowed some passage of both fish and water. High river flows in 2011 and 2017 prevented barrier installation in those years, and it was also not installed in 2013. In 2009 and 2010, it was replaced with an experimental nonphysical barrier (bioacoustic fish fence) that used light and a bubble curtain to deter fish from entering OR (Bowen and Bark 2012).

Tagging Study

Each year from 2009 to 2017, between 504 and 1,875 juvenile hatchery-raised subyearling fall-run Chinook Salmon were surgically tagged with microacoustic transmitters (hereafter, "tags") and released into the SJR at Durham Ferry, located approximately 118 rkm upstream of Chipps Island and 21 rkm upstream of Mossdale. Fish were sourced from the Feather River Fish Hatchery in 2009, the Mokelumne River Hatchery in 2014, and the Merced River Hatchery in all other years. Fish size at tagging ranged from 73 to 140 mm and averaged 85.1–115.3 mm per year (Table 2). The tag and receiver technology changed over the course of the study: HTI in 2009–2011, Vemco in 2012–2016, and the Juvenile Salmon Acoustic Telemetry System (JSATS) in 2017 (Table 2). Although different years involved the use of different technology, consistent study design and data processing methods were implemented to ensure comparable ability to estimate survival throughout the Delta. Tag life studies were conducted each year to detect manufacturing faults and allow for modeling of tag survival through time; mean tag life ranged from 27.3 d in 2010 to 50.6 d in 2013. Additional details on the surgical, handling, and release procedures are available in Buchanan et al. (2018) and the annual technical reports (SJRGA 2010, 2011, 2013; Buchanan et al. 2015, 2016, 2018; Barnard et al. 2022; Towne et al. 2022). In some study years, additional fish were released at intermediate locations between Durham Ferry and Chipps Island; those releases are not included here. The 2015 study is omitted from this work because extreme drought during that year compromised the fish release at Durham Ferry.

Acoustic receivers were placed at key sites ("telemetry stations") throughout the Delta (Table 3; Figure 1). Each year, telemetry stations were located in the SJR just downstream of the HOR (river junction) near Lathrop, California (SJL station), and just downstream of the Turner Cut

TABLE 2. Summary of annual tagging studies of juvenile hatchery fall-run Chinook Salmon. All fish were released at Durham Ferry on the San Joaquin River (N = number released). Fork length (mm) is the mean at tagging, with range shown in parentheses. Tag burden is tag weight calculated as a percentage of fish weight (JSATS = Juvenile Salmon Acoustic Telemetry System). Water year classification (WY type) is presented either as defined by the California Department of Water Resources (CDWR; cdec.water.ca.gov/reportapp/javareports?name=WSIHIST) or as used in this analysis. The "HOR barrier" indicates the type of temporary barrier used at the head of Old River during the tagging study (NPB = nonphysical barrier; PB = physical barrier [rock]).

Year	Release dates	N	Hatchery	FL (mm)	Tag type	Tag burden (%)	WY type (CDWR)	WY type (analysis)	HOR barrier
2009	Apr 22–May 13	933	Feather River	94.8 (85–110)	HTI Model 795	7.1 (4.4–10.2)	Below normal	Normal	NPB
2010	Apr 27–May 20	504	Merced	110.5 (99–121)	HTI Model 795	4.2 (2.8–5.7)	Above normal	Normal	NPB
2011	May 17–Jun 19	1,895	Merced	110.8 (94–140)	HTI Model 795	4.1 (2.0–6.5)	Wet	Wet	None
2012	May 2–22	959	Merced	112.7 (100–135)	Vemco V5, 180 kHz	3.8 (2.0–5.4)	Dry	Dry	PB
2013	May 1–19	950	Merced	115.3 (101–135)	Vemco V5, 180 kHz	3.8 (2.4–5.2)	Critical	Dry	None
2014[a]	Apr 30–May 19	1,275	Mokelumne	98.9 (88–119)	Vemco V4, 180 kHz	3.8 (2.1–5.0)	Critical	Dry	PB
2016	Apr 13–22	648	Merced	85.1 (73–98)	Vemco V4, 180 kHz	5.8 (3.4–7.0)	Dry	Dry	PB
2017	Apr 12–30	647	Merced	89.5 (77–110)	JSATS	3.5 (1.9–5.0)	Wet	Wet	None

[a]A release group of 643 Chinook Salmon from mid-April 2014 was omitted because of tag programming error.

Junction (TCJ; river junction) at MacDonald Island (MAC station). A telemetry station was also located in Turner Cut (TRN station). Stations were placed in OR near its head (ORE station) and near the Highway 4 bridge north of the water pumping facilities (OR4 station). Stations were also placed in MR near Highway 4 (MR4 station), at the entrance of the CVP and in the holding tanks (collectively, the CVP station), and at the entrance of the Clifton Court Forebay (CCF station) outside the state water pumping plant (Figure 1). In all years except 2009, a telemetry station was located at the Delta exit at Chipps Island (CHP station).

Data Processing

Detection data were processed by Natural Resource Scientists, Inc. (Red Bluff, California; 2009, 2010), or by the U.S. Geological Survey (USGS), Sacramento, California office (2011–2017) and then were transferred to either the University of Washington (2009–2014) or the USGS Great Lakes Science Center (2016, 2017) for further analysis. The receiver data were converted to detection events and reviewed for possible detections of predators that had eaten the tagged study fish. Likely predator detections were identified using a rule-based predator filter based on residence time in the vicinity of the telemetry stations, migration rate through the study area, movements directed against river flow, and regional movement patterns deemed unlikely for salmon smolts (SJRGA 2013; Buchanan and Whitlock 2022). Detection histories were constructed for each tag in a space-for-time multistate mark–recapture model (Skalski et al. 1998; Hance et al. 2020), indicating the stations where each tag was detected; in the event of multiple detection events at the same station or river junction, the final passage of the location was used in the detection history. Estimates of conditional detection probabilities (i.e., detection efficiencies) were computed for each release group from a mark–recapture model that used all available detection data (Supplemental Table S1 available in the online version of this article); more information is available in the annual reports on the tagging studies, data processing, and mark–recapture analysis (SJRGA 2010, 2011, 2013; Buchanan et al. 2015, 2016, 2018; Barnard et al. 2022; Towne et al. 2022). The analysis presented here used the tags detected at the SJL and ORE telemetry stations to define virtual release groups for survival modeling through reaches downstream of those stations. All data processing and analysis were performed using R version 3.6.0 (R Core Team 2019).

Covariate Data

The covariates considered in the modeling exercise were selected based on a combination of the conceptual model, management interests, and variables found to be significant in the initial modeling exercise presented by Buchanan and Skalski (2020; Table 4). Water project operations in the Delta use a number of metrics as management tools

TABLE 3. Geographic acronyms and site names, including type and location indicated by river kilometers (rkm) measured from the Golden Gate Bridge (entrance to the Pacific Ocean). Distances to sites on the San Joaquin River (SJR) are measured along the main stem of the river.

Name	Type	Description[a]	rkm
CV	Region	Central Valley of California	
FH4	Region	Interior Delta region at water export facilities and Highway 4, bounded by telemetry stations CVP, CCF, MR4, and OR4	
MR	River	Middle River	
OR	River	Old River	
SJR	River	San Joaquin River	
TC	Channel	Turner Cut	
HOR	River junction	Head of Old River	171
TCJ	River junction	Turner Cut Junction	137
DF	Release site	Durham Ferry	195
CCF	Telemetry station	Clifton Court Forebay	142
CHP	Telemetry station	Chipps Island	77
MAC	Telemetry station	MacDonald Island	134
MR4	Telemetry station	MR at Highway 4	137
OR4	Telemetry station	OR at Highway 4	134
ORE	Telemetry station	OR near head	164
SJL	Telemetry station	SJR at HOR	170
TRN	Telemetry station	Turner Cut	138
CVP	Telemetry station; water export facility	Central Valley Project	144
SWP	Water export facility	State Water Project	146
MID	Gauging station	MR at Bacon Island (USGS 11312676)	126
ORB	Gauging station	OR at Bacon Island (USGS 11313405)	123
SJG	Gauging station	SJR at Garwood Bridge (CDEC SJG)	150
SLT	Gauging station	SJR at Lathrop (Water Data Library B95765)	170
VNS	Gauging station	SJR at Vernalis (Dayflow SJR)	198

[a]Database source and site identification number are identified for gauging stations (USGS = U.S. Geological Survey; CDEC = California Data Exchange Center).

designed to support survival of smolts migrating from the SJR, including SJR discharge measured near Vernalis, California (VNS; Table 3; referred to as "Delta inflow"); the daily export pumping rate from one or both of the water export facilities (CVP or SWP; "exports"); the ratio of Delta inflow to the daily export pumping rate (IE; inflow : export ratio [I:E ratio]); and measures of river flow in the interior Delta region north of the water export facilities (ORB = OR at Bacon Island, MID = MR at Bacon Island, or OMT = ORB + MID; "interior Delta flow"; Figure 1). Some of these metrics stood out as important for explaining variability in survival in the 2010–2014 model described by Buchanan and Skalski (2020), such as the interior Delta flow measures, the CVP export rate, and the I:E ratio. Other important measures from that exercise were SJR water temperature measured at Lathrop (SLT monitoring station) and the SJR discharge at Garwood Bridge (SJG; Figure 1; Table 3), which were relevant for modeling survival from Lathrop to the TCJ (Buchanan and Skalski 2020). The estuarine salinity metric X2 (location where salinity concentration at the river bottom reaches 2‰; Jassby et al. 1995) was also identified as associated with survival between Lathrop and the TCJ but was omitted here because of poor overlap in observed values between years. Export rates were characterized by the CVP and SWP measures separately for modeling total survival to Chipps Island because of possible differences in facility mortality, including predation in the reservoir outside of the state pumping plant (Figure 1; Table 4). For the upstream survival models, exports were characterized by the combined export rate (CVP + SWP) because without a mechanism directly tied to either water export facility (e.g., CVP salvage), it was expected that the routing and hydrodynamic effects of the total export operations would be more relevant to survival than the operations of either facility alone.

Estimates of total Delta outflow at Chipps Island (QOUT) were used to model detection probabilities at the CHP telemetry station. Also included in this analysis were fish size (FL at tagging), route selection at the HOR, and the presence of the physical (rock) barrier at the HOR. The physical barrier status was included because of the potential for the rock barrier to intensify net positive flows

TABLE 4. Covariates evaluated in updated (2009–2017) individual-based models or in assessment of old (2010–2014) models. "Station" lists the gauging station, monitoring station, or water export facility; see Figure 1 for locations (OMT = ORB + MID; codes are defined in Table 3). Summary period (duration in days) started at detection at the SJL or ORE telemetry station. Metrics are daily (daily measure or average daily mean), net (average net flow), root mean square (RMS), or average (average of 15-min event data). Survival models that used the covariate are noted (A = assessment of 2010–2014 models; X = 2009–2017 models; P = detection probability model at the downstream telemetry station).

Name	Type	Station	Duration (d)	Metric	Units	HOR–CHP	SJL–TCJ	ORE–FH4
CVP.2	Exports	CVP	2	Daily	m^3/s	AX		
CVPSWP.2	Exports	CVP + SWP	2	Daily	m^3/s		X	X
FL at tagging	Fish size				mm	X	X	X
IE.2	Inflow: export ratio[a]	VNS, CVP, SWP	2	Daily		AX	X	X
MID.1net	Flow	MID	1	Net	m^3/s		A	
MID.2net	Flow	MID	2	Net	m^3/s	A		
MID.3net	Flow	MID	3	Net	m^3/s	X		
OMT.1net	Flow	OMT	1	Net	m^3/s		AX	X
OMT.2net	Flow	OMT	2	Net	m^3/s	A		
OMT.3net	Flow	OMT	3	Net	m^3/s	X		
OMT.1rms	Flow	OMT	1	RMS	m^3/s			X
OMT.3rms	Flow	OMT	3	RMS	m^3/s	X		
ORB.1net	Flow	ORB	1	Net	m^3/s		A	
ORB.3rms	Flow	OMT	3	RMS	m^3/s	AX		
Physical barrier	Barrier				T/F	X	X	
QOUT	Delta outflow	CHP[b]	1	Daily	m^3/s	P		
Route	Migration route				SJR/OR	X		
SJG.1net	Flow	SJG	1	Net	m^3/s		AX	
SWP.2	Exports	SWP	2	Daily	m^3/s	X		
Tslt.2	Temperature	SLT	2	Average	°C	X	AX	X
VNS.2	Flow (Delta inflow[a])	VNS	2	Daily	m^3/s[a]	X	X	X
WY type[b]	Water year type				Dry, normal, wet	X	X	X
Year	Calendar year				Categorical	X	X	X

[a]Transformed to the $\log_e$ scale.
[b]As reported in the California Department of Water Resources Dayflow database (water.ca.gov); measured on observed date of tag detection at the CHP telemetry station for detected tags or measured 6 d (3 d) after detection at SJL (ORE) for nondetected tags.

in the SJR and net negative flows in the OR downstream of the HOR; the barrier status changed on an annual basis. The nonphysical barrier status (on versus off; 2009, 2010) was not considered here because the virtual release sites (SJL and ORE) were downstream of the barrier and hydrodynamics were unlikely to be strongly affected by the operation of the nonphysical barrier.

Environmental and operational data from several gauging and monitoring stations were downloaded from four online databases: CDWR's Dayflow database (data.cnra.ca.gov/dataset/dayflow; Delta inflow and outflow, export rates), the California Data Exchange Center (cdec.water.ca.gov; river discharge at SJG), the California Water Data Library (water.ca.gov/waterdatalibrary; temperature), and the USGS National Water Information System (water.data.usgs.gov/nwis; river discharge at ORB and MID). River discharge and temperature data were reviewed for quality, and obvious errors were omitted; records were removed if they were out of sequence with neighboring readings or were part of a string of three or more identical readings (discharge only).

Environmental and operational data were downloaded as either daily measures (export rates, Delta inflow and outflow) or 15-min event data (discharge, temperature) and were summarized over time periods relevant to conditions representing the majority of tagged fish movement in the Delta. Each summary period began at the time of tag detection at the HOR telemetry stations (SJL or ORE). As in Buchanan and Skalski (2020), the measures of Delta inflow and export rates, I:E ratio, and temperature were summarized as 2-d means starting at the time of HOR detection in order to represent conditions that all fish experienced in the upstream region of the study area (Table 4). Measures of river discharge in the interior Delta and at the SJG gauging station were summarized over 1- and 3-d periods starting at HOR detection; 1-d periods were used to model survival in the upstream reaches of the study area, and 3-d periods were used to model through-Delta survival (HOR–CHP). Two-day periods were used for some gauging stations in assessment of the 2010–2014 model. Discharge summaries were the average net discharge (SJG and interior Delta measures) and the root mean square (RMS; interior Delta measures). The average net discharge represented a combination of water volume, velocity, and flow direction (downstream is >0 and upstream is <0), whereas the RMS measure represented the average volume of discharge without the effects of reverse flows or tidal and diurnal influences. Average net flow measures tend to vary about 0 in tidally influenced areas, whereas RMS values are always greater than 0. As in Buchanan and Skalski (2020), estimated Delta outflow was recorded on the day of tag detection at the CHP telemetry station or on the expected day of arrival for tags that were not detected there. The expected arrival day was defined as 6 d after detection at SJL or 3 d after detection at ORE based on median travel times observed for the two routes (5.7 and 2.6 d, respectively).

Assessment of 2010–2014 Model Fit

The model previously defined for years 2010–2014 was a generalized linear model (GLM) using a logit link, where the survival probability was modeled as

$$\operatorname{logit}(S_{iy}) = \beta_{0y} + \beta_1 x_i \tag{1}$$

for covariate x, individual i in year y; and where logit$(\cdot)$ is the logit link function and β_{0y} and β_1 are the fixed effects of year y and covariate x, respectively (Buchanan and Skalski 2020). For the reach from the SJL station near the HOR to the TCJ (MAC and TRN stations), the GLM was a known-fate model using binomial errors and the assumption that detection probability was equal to 1.0 at the MAC and TRN stations. For the reach from the HOR (ORE and SJL stations) to Chipps Island (CHP station), the GLM was a release–recapture model using multinomial errors. Detection probability at CHP was modeled as

$$P_i = 1-(1-P_{1i})(1-P_{2i}), \tag{2}$$

where P_{ji} is the probability of detection on receiver line j $(j = 1, 2)$ given presence at that line, modeled as

$$\operatorname{logit}(P_{ji}) = \gamma_0 + \gamma_1 \mathrm{QOUT}_i \tag{3}$$

for fixed effects γ_0 and γ_1 and Delta outflow (QOUT_i) for individual i. Tag survival was included as a release-group-level offset (Buchanan and Skalski 2020).

Assessment of predictions from the model in equation (1) with new data is complicated by use of fixed year effects β_{0y} in equation (1), which prevents direct comparison of predicted absolute survival with observed survival for out-of-sample years—that is, those years not used in the original model construction (2009, 2016, and 2017). However, equation (1) assumes a common relative relationship for all years between covariate x and survival regardless of the fixed year effects (i.e., shared slope terms). Thus, if the dynamics represented in the previously fitted model hold for out-of-sample years, then a similar relative relationship between covariate levels and survival should be observed for those new years (Wenger and Olden 2012). Because the model uses a logit link, β_1 represents the change in the log odds of survival for a unit change in x or, equivalently, the log odds ratio (LOR) between two values of x. The fit of the old model to new data can be assessed by comparing the model's prediction of the relative odds of survival for a range of covariate values to a baseline case with the observed ratios of performance using the new data; this can be done even for years in which conditions lie beyond the range of the original data. This approach was implemented by classifying records of individual fish into "bins" based on their observed covariate values and then computing the LOR of survival, comparing each bin to a baseline bin (described below). Binning is a common approach in assessment of categorical models (e.g., Hosmer and Lemeshow 2000) and also facilitates out-of-sample assessment of the year effects model. If there is no association between survival and the covariate, then the LOR should be zero. A positive association between the covariate and survival is indicated by an LOR greater than 0 and a monotonically increasing sequence of LOR values for consecutive bins compared against a low baseline bin; likewise, a negative association between the covariate and survival is indicated by an LOR less than 0.

For covariate x, the individual tags $i = 1, \ldots, n$ were ranked by their associated observations of x $(x_1, \ldots, x_n)$ and were assigned to bins of approximately equal size (i.e., subdivided by quantiles). For example, in the 2017 assessment of the SJG flow model, the tags from 2017 were ranked by their observed SJG flow values and were assigned to six bins of 33–38 tags each. The target minimum bin size was 30 individuals; between four and six bins were used for each model assessment, depending on the reach, year, and covariate. Bins were numbered $b = 0, \ldots, B-1$, where $b = 0$ indicates the bin with the lowest covariate values; the observations of covariate x in bin b were $x_{b1}, \ldots, x_{bm}$. For each bin $b > 0$, the LOR comparing bin b to bin 0 was predicted from the existing model (equation 1) as

$$\widetilde{\mathrm{LOR}}_b = \tilde{\beta}_1(\bar{x}_b - \bar{x}_0),$$

where the tilde ("~") notation indicates estimates from the existing model (equation 1) and $\bar{x}_b$ is the mean of new observations of covariate x in bin b ($b = 0, \ldots, \mathrm{B}-1$). An asymptotic 95% confidence interval was computed as $\tilde{\beta}_1 \pm 1.96\sqrt{\widehat{\mathrm{Var}}\left(\widetilde{\mathrm{LOR}}_b\right)}$, where $\widehat{\mathrm{Var}}\left(\widetilde{\mathrm{LOR}}_b\right)$ was computed using the law of total variance (see Supplemental Materials available in the online version of this article for details).

The predicted LOR from the existing model was compared to the estimated (i.e., observed) LOR for bins 0 and $b > 0$ for each out-of-sample year, where the observed LOR was computed based on the relative frequency of observed detections at the reach's downstream telemetry stations for bin b compared to bin 0. The observed LOR is equivalent to the estimated effect of bin b relative to the baseline bin (i.e., $\hat{\beta}_b$) in the individual-based binomial GLM:

$$\mathrm{logit}(S_i) = \beta_0 + \beta_b I_{ib}, \tag{4}$$

where I_{ib} is an indicator function that has a value of 1 if x_i is contained in bin b and has a value of 0 otherwise. For the HOR–CHP reach, we accounted for detection probability at the CHP telemetry station by adjusting the detection outcome (1 or 0) for each tag by the predicted detection probability for that tag using the 2010–2014 detection probability model in equations (2) and (3). Tag survival was accounted for in a similar manner using the estimated tag survival curve for the tag life study from the out-of-sample year.

The baseline bin was selected as the lowest-valued bin for which a positive number of successes (i.e., downstream detections) was observed; this was bin 0 for all covariates. Fit of the existing model (equation 1), previously estimated using data from the years 2010–2014, was assessed for the out-of-sample years by inspecting the membership of the new observed LOR values ($\hat{\beta}_b$ from equation 4) within the 95% confidence intervals from the model-predicted LORs and determining whether the pattern of observed LOR values across multiple bins agreed well with the pattern of predicted LOR values. Poor model fit was concluded if the observed LOR values fell far outside the model bounds and either trended differently from the modeled trend (i.e., different slopes) or showed no trend (i.e., no linear association) combined with imprecise β_b estimates from equation (4) (i.e., wide confidence intervals). Because the three out-of-sample years represented three different WY types (Table 2), model assessment was performed for each out-of-sample year separately.

For the reach from SJL to TCJ, the fit of the 2010–2014 model to out-of-sample data from 2009, 2016, and 2017 was assessed for the top-ranked flow and temperature covariates identified by Buchanan and Skalski (2020): OMT.1net, MID.1net, ORB.1net, and Tslt.2 (covariates are defined in Table 4). We also investigated the top-ranked SJR flow metric, SJG.1net. For each covariate, the bin that contained the lowest observed values of the covariate for the year was used as the baseline bin.

For the reach from the HOR to Chipps Island (HOR–CHP), model fit was assessed for the top covariate identified by Buchanan and Skalski (2020), ORB.3rms, as well as the top net MID and OMT flow covariates, MID.2net and OMT.2net, and the top exports covariate, CVP.2. The I:E ratio covariate, IE.2, was also included because it had a significant effect in Buchanan and Skalski (2020) and is of management interest. For each covariate, the baseline was the bin that contained the lowest observed values of the covariate. Model fit was assessed only for 2017; no receivers were deployed at Chipps Island in 2009, and although receivers were deployed at Chipps Island in 2016, no tags were detected there, thus preventing model assessment using relative survival.

Development of New Models

The models in Buchanan and Skalski (2020) used fixed year effects to capture annual differences that were unrelated to the model's covariate. More useful for management would be models that included effects of the yearly "WY type" rather than calendar year effects per se. Water year type is a hydrological classification of annual runoff to upstream lakes and reservoirs in the SJR basin before adjustments by diversions or water transfers to or from other river systems; it is used by managers for various purposes, including setting targets for reservoir releases and water export rates (Table 2). In the initial analysis by Buchanan and Skalski (2020), there was too little replication of WY types to develop a useful model. With the expanded data set, it is now more reasonable to develop a WY type model. The inclusion of 2017 in particular provides a valuable second "wet" year, which is especially helpful because of the suspected leverage exerted by what was previously the only wet year (2011). Even using the expanded data set, there are five different management-defined WY types observed among the 8 years of the study. For the purposes of this analysis, it was necessary to combine similar WY types to form a simpler classification: wet, normal, and dry, where "normal" consists of the "above normal" and "below normal" management classifications and "dry" consists of the "dry" and "critical" management classifications. This "analysis" classification resulted in two wet years, two normal years, and four dry years (Table 2).

The potential benefit to survival from remaining in the SJR at the HOR is an ongoing management question, as is the effect of a physical barrier at the HOR. Although not a primary focus of the analysis, survival is thought to be positively influenced by fish size (Evans et al. 2014). Thus, fish size, the presence of a physical barrier, and migration route were included as fixed effects in all models, depending on the reach and type of year effects (described more fully below).

The new models for the HOR–CHP and SJL–TCJ reaches were assessed both with and without the 2011 study year to examine the sensitivity of the original modeling results on the single year that provided the majority of the data in the earlier modeling exercise (2010–2014). The new models were first constructed using all available years; the top-ranked models were then refit to the data without the 2011 study year.

Head of Old River to Chipps Island.— Survival from the HOR to Chipps Island ($S_{\text{HOR–CHP}}$) was modeled using an approach similar to that taken in Buchanan and Skalski (2020). The joint processes of survival and detection were modeled using an individual-based mark–recapture framework in a GLM with multinomial errors and logit link for both survival and detection. The multinomial framework was selected to account for the possibility of nondetection at the CHP station, even for successful migrants. The conditional probability of detection at CHP was modeled using the pattern of detections at the CHP dual array as in equations (2) and (3). Tag failure was accounted for by using group-level offsets equal to the estimated probability of tag survival to Chipps Island for the modeled year and migration route; estimated tag survival probabilities were 0.96 or greater.

The probability of survival to Chipps Island was modeled as a function of group-level factors and individual-level covariates. Group factors were WY type (dry, normal, or wet), migration route (SJR or OR), and the presence of the physical barrier at the HOR (present or absent). Preliminary analyses found no benefit to explanatory value in modeling an interaction effect between barrier and either route or WY type, so only main effects were used. Fork length was included in all models to account for size differences between years (Table 2). The effects of the remaining covariates were assessed in single-variable models of the form

$$\text{logit}(S_{wrbi}) = \beta_{0w} + \rho I_r + \tau I_b + \beta_L L_i + \beta_1 x_i, \qquad (5)$$

where β_{0w} is the baseline intercept for WY w (SJR route, no physical barrier); ρ and τ are intercept adjustments and I_r and I_b are indicator functions for the OR route and the presence of the physical barrier, respectively; β_L is the slope (regression coefficient) for FL; L_i is FL for fish i; and β_1 and x_i are the slope and observed value, respectively, of covariate x for fish i. The explanatory utility of individual environmental and operational variables (x) was assessed using F-tests. Main effects were evaluated for each variable. Interaction effects were assessed between Delta inflow (VNS.2) and the physical barrier, between route and the top interior Delta flow variable, and between route and the top exports variable. Akaike's information criterion (AIC; Burnham and Anderson 2002) was used to compare models using different environmental and operational variables. The single-variable model with the lowest AIC was used as a basis for adding a second environmental or operational variable. Goodness of fit was represented by examining the area under the curve (AUC) for the receiver operating characteristic curve (Nam and D'Agostino 2002); values of AUC greater than 0.7 were considered acceptable (Hosmer and Lemeshow 2000).

The dependence of HOR–CHP survival on migration routing at the HOR under different environmental and operational conditions was assessed by comparing the predicted survival in the SJR route to the OR route using the single-variable regression models for Delta inflow (VNS.2) and the top-ranked metrics for both exports and interior Delta flow. Route-specific survival was compared within each of the three WY types (dry, normal, and wet) for fish of average FL (107 mm) and for the predominant observed barrier conditions within that WY type. For the "dry" WY scenarios, survival was predicted with the physical barrier in place for the SJR route and without the physical barrier for the OR route. Survival was predicted without the physical barrier for the "normal" and "wet" settings, reflecting the observed combinations of WY type and barrier in the data; additionally, high flows prevent the installation of the physical barrier during wet years. The route or barrier interaction models were used as the basis of comparison. Asymptotic 95% prediction bands were calculated for each survival curve.

Lathrop to Turner Cut Junction.— The probability of survival from Lathrop (SJL) to the TCJ, $S_{\text{SJL–TCJ}}$, was modeled as a function of covariates using an individual-based GLM with binomial errors and logit link function (Buchanan and Skalski 2020). Successful survival to the TCJ was denoted by detection on either the TRN or MAC telemetry station. Drawing inference to survival separately from detection depended on 100% conditional detection probabilities at TRN and MAC (i.e., all tagged salmon present at the stations were actually detected there). Estimated detection probabilities at these stations were consistently high (≥0.97; Supplemental Table S1), so making inference to survival was justified. Similar to the survival models for the HOR–CHP reach, the SJL–TCJ models used fixed effects of both group-level and individual-level covariates. All models included WY type, the presence of the physical barrier, and FL at tagging. The association between survival and other individual-level covariates was explored for covariates related to management strategies and those found to be important in the 2010–2014 investigation (Buchanan and Skalski 2020): Delta inflow (VNS.2), combined export rate (CVPSWP.2), I:E ratio (IE.2), SJR water temperature at Lathrop (Tslt.2), and the 1-d average net interior Delta flow combined over the OR and MR stations (OMT.1net; Table 4). The 1-d average net SJR flow at the SJG gauging station (SJG.1net) was also found to have a significant effect in Buchanan and Skalski (2020) but was missing all observations from 2014. The effect of SJG flow was assessed for the remaining years and was compared to the top model identified from the full data set. Estimated tag survival to the TCJ was at least 0.99 for all tags, so no adjustments were made for premature tag failure. The methods of model construction, selection, and goodness-of-fit testing for SJL–TCJ were the same as those used for HOR–CHP modeling.

Head of Old River to facilities and Highway 4.— The survival process was investigated between the ORE telemetry station, located in OR near its head, and the interior Delta region near the water export facilities and Highway 4 (FH4 region). Survival through this region ($S_{\mathrm{ORE-FH4}}$) was denoted by detection on any of the telemetry stations located at the CVP, the CCF, or Highway 4 (OR4 and MR4; Figure 1). Because of the complicated migration routing choices required by salmon in this region, detections from these four detection sites were pooled. Inference to survival required assuming 100% conditional detection probabilities at these four sites (i.e., $P_{\mathrm{CVP}} = P_{\mathrm{CCF}} = P_{\mathrm{OR4}} = P_{\mathrm{MR4}} = 1$). Detection probabilities could not always be estimated for individual release groups or annual groups because of sparse detections in the OR route; however, the available estimates were all 0.95 or greater and most were equal to 1.00 (Supplemental Table S1). The same model structure and covariates were used as in the SJL–TCJ investigation, with the exclusion of the SJG flow metric and the addition of the 1-d RMS of interior Delta flow at OMT (OMT.1rms). The model construction, selection, and goodness-of-fit methods were the same as those used for the SJL–TCJ and HOR–CHP modeling.

RESULTS

Virtual release size at the HOR stations ranged from 9 tags at ORE in both 2012 and 2016 to 919 tags at SJL in 2011, and detection counts at CHP ranged from 0 in both 2014 and 2016 to 31 in 2011 (Table 5). Most fish detected at the TCJ were observed taking the SJR route from there, indicated by detection at the MAC telemetry station. Among the OR route fish detected at the water facilities or Highway 4 sites (FH4 region), most were detected at either the CVP or CCF station rather than the Highway 4 stations; very few were observed at the MR4 station (Table 5).

Most covariate values were loosely stratified by WY type, with notably higher values of Delta inflow (VNS.2), CVP exports, I:E ratio, and average net measures of interior Delta flow (e.g., OMT.3net) seen in the very wet year of 2017 compared to the other years. There was more overlap in covariates among the normal and dry WY types, with the exception of VNS.2, which was lowest for the dry years (Figure 2). The highest degree of overlap among all WY types was observed for the RMS measures of interior Delta flow (e.g., OMT.3rms and ORB.3rms; Figure 2; Supplemental Figures S1, S2 available in the online version of this article).

Assessment of 2010–2014 Model Fit

Lathrop to Turner Cut Junction.— Using the bin with the lowest observed covariate values as the baseline, the predicted LOR values from the 2010–2014 model increased slightly for higher-valued bins for the flow covariates and decreased for higher bins of temperature (central horizontal bars in Figure 3A, Supplemental Figure S3). The change in predicted LOR from one bin to the next depended both on the estimated regression coefficient β and the average observed covariate values in the adjacent and baseline bins. Under the hypothesis that the model captures the dynamics in the out-of-sample year, the observed LOR values (i.e., $\hat{\beta}_b$ from equation 4) should follow the same pattern as the model-predicted values and ideally should be contained within the 95% confidence interval of the predicted LOR values (white boxes in Figure 3A, Supplemental Figure S3); very wide observed confidence intervals compared to modeled intervals indicate poor model fit.

The model predictions of LOR for 2009 showed poor agreement with the observed LOR values for all covariates considered (Figure 3A; Supplemental Figures S3, S4). At most, one LOR value (of three or five, depending on the covariate) was contained within the predicted confidence interval for any covariate, the pattern of observed LOR values did not match the expected monotonic pattern for any of the covariates, and the observed confidence intervals were very wide in comparison to the predicted ranges. The bin sample size was 36–39 for the flow covariates (56 for temperature), and only 17 tags were detected at the TCJ out of the 224 tags in the virtual release group at SJL (Table 5), resulting in low survival estimates and increased sensitivity of the LOR values to bin membership. It appears that the 2010–2014 models did not reflect the 2009 dynamics well.

The 2010–2014 model fit the 2016 data better than the 2009 data according to the observed and predicted LOR values, although there remained wide observed confidence intervals and noticeable differences between the pattern of predicted and observed LOR values for the interior Delta flow metrics (Figure 3A; Supplemental Figures S3, S4). The SJG.1net model agreed with the observed LOR values for the higher SJG.1net bins (compared to the lowest bin as baseline), and a nearly monotonic decreasing pattern of observed LOR values was observed for

TABLE 5. Detection counts at telemetry stations for each study year. Telemetry stations are identified in Figure 1, and codes are defined in Table 3 (NA = not available; the Chipps Island [CHP] station was not installed in 2009).

Year	Upstream station	Upstream count	CHP	MAC	TRN	CVP	CCF	OR4	MR4
2009	SJL	224	NA	16	1				
	ORE	283	NA			78	70	12	0
2010	SJL	202	9	75	6				
	ORE	228	19			64	52	58	0
2011	SJL	919	6	348	95				
	ORE	656	25			139	184	103	3
2012	SJL	443	14	97	12				
	ORE	9	1			3	0	1	0
2013	SJL	106	1	2	0				
	ORE	341	2			62	17	15	3
2014	SJL	101	0	1	2				
	ORE	9	0			2	0	0	0
2016	SJL	245	0	22	3				
	ORE	32	0			2	1	3	0
2017	SJL	215	5	94	9				
	ORE	173	8			24	38	44	10

temperature (Tslt.2), as predicted from the model. Similar to 2009, there were few detections at the TCJ stations in 2016 (25 of the 245 tags detected at SJL); bin size was 40–42 tags.

The 2017 study year showed the highest level of agreement with the 2010–2014 model predictions despite the observed covariates from 2017 largely falling beyond the range of the original 2010–2014 data. Between two and five observed LOR values (out of five possible) fell within the predicted ranges for all flow covariates (Figure 3A; Supplemental Figures S3, S4). The SJG.1net model predictions showed the best agreement with observed values, and the temperature (Tslt.2) model exhibited the worst agreement (Supplemental Figure S3). Despite some limitations in the predictive power of the 2010–2014 model for 2017, it appeared to perform better for that year than for either 2009 or 2016. The year 2017 was a wet year, as was 2011, which was the source of the majority of records used in fitting the 2010–2014 models. The improved model fit of 2017 compared to the drier years suggests that the existing model may be considered a “wet year model,” despite including up to three drought years.

Head of Old River to Chipps Island.— The 2017 model assessment for the reach from the HOR to Chipps Island also used the bin with the lowest-valued covariates observed as the baseline for each covariate. The predicted LOR values from the 2010–2014 model increased with increasing covariate bins for the ORB.3rms and CVP.2 models (central horizontal bars in Figure 3B) and decreased for higher covariate bins for the MID.2net, OMT.2net, and IE.2 models (Supplemental Figure S5). The model predictions of LOR showed better agreement with observed LOR patterns for the ORB.3rms and CVP.2 models than for the net interior Delta flow models or the I:E ratio model (Figure 3B; Supplemental Figure S5). Observed LOR confidence intervals were typically smaller than the predicted intervals for all covariates, and the observed LOR point estimates fell within the predicted interval for 12 of the 18 bins with observations. Of the six bins with no LOR observed (i.e., no tags detected at CHP), three were consistent with patterns of reduced survival compared to the baseline bin, as predicted from the model (Supplemental Figure S5).

The observed values of both CVP.2 and IE.2 were not evenly distributed, and a large number of tied covariate values resulted in uneven bin sizes ranging from 36 to 103 for these two metrics (bin sizes = 64–65 for other covariates). Considering the uneven bin size and low survival predicted overall, the predictions from the 2010–2014 model may be considered mostly consistent with observed detection patterns from 2017.

New Models

Head of Old River to Chipps Island.— Detection counts at CHP ranged from 0 (2014, 2016) to 14 for SJL fish (2011) and 25 for ORE fish (2011; Table 5). Detection probabilities at the CHP telemetry station (P_{CHP}) were 0.95 or greater for all releases except the May 2011 group, which had a $\hat{P}_{CHP}$ of 0.75 (Supplemental Table S1).

There was moderate support for the survival model that used the 3-d RMS of interior Delta flow measured at ORB ($P = 0.046$; Table 6). A positive association was observed

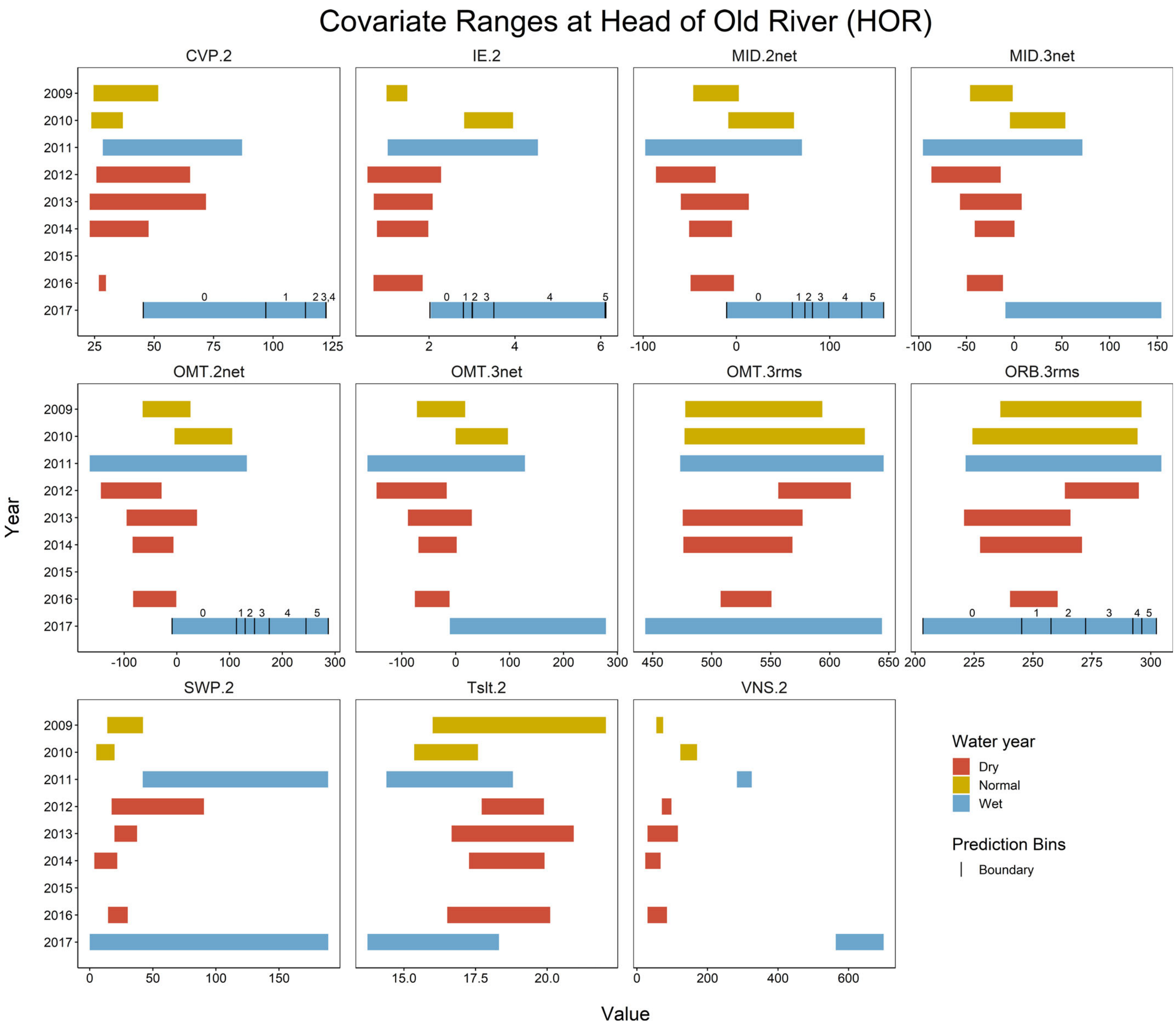

FIGURE 2. Observed ranges of covariates used in assessment of the 2010–2014 model or in construction of the new model of Chinook Salmon smolt survival from the head of Old River (HOR) for each study year, color-coded by water year type (red = dry; gold = normal; blue = wet). Vertical bars for 2017 indicate boundaries of prediction bins used in assessment of the 2010–2014 model of survival from HOR to Chipps Island; numbers 0–5 above bins indicate the bin labels. Bin 0 was the reference bin used in computing the odds ratio for model assessment. Covariates are defined in Table 4.

after adjusting for WY type (Figure 4), and an interaction with route was not indicated ($P = 0.67$). A similar relationship was observed with the 3-d RMS of OMT flow. There was weaker support for survival relationships with all other covariates ($P = 0.095$ for CVP export rate, $P \geq 0.12$ for all others; Table 6). Although the slope of the Delta inflow (VNS.2) term was higher (>0) when the physical barrier was in place, the difference was not significant ($P = 0.42$). No secondary covariates were associated with survival after adjusting for ORB.3rms ($P \geq 0.31$). The AUC values of the single-covariate models ranged from 0.72 to 0.78, indicating acceptable model fit (Table 6). The baseline model that adjusted for WY type, migration route, physical barrier, and FL had an AUC of 0.73, whereas the null survival model that accounted for no group- or individual-level covariates had an AUC equal to 0.48.

The 3-d RMS of ORB flow remained the top covariate, and its estimated association with survival (i.e., slope) remained greater than 0 when the 2011 data were omitted, although the reduction in the total degrees of freedom (df

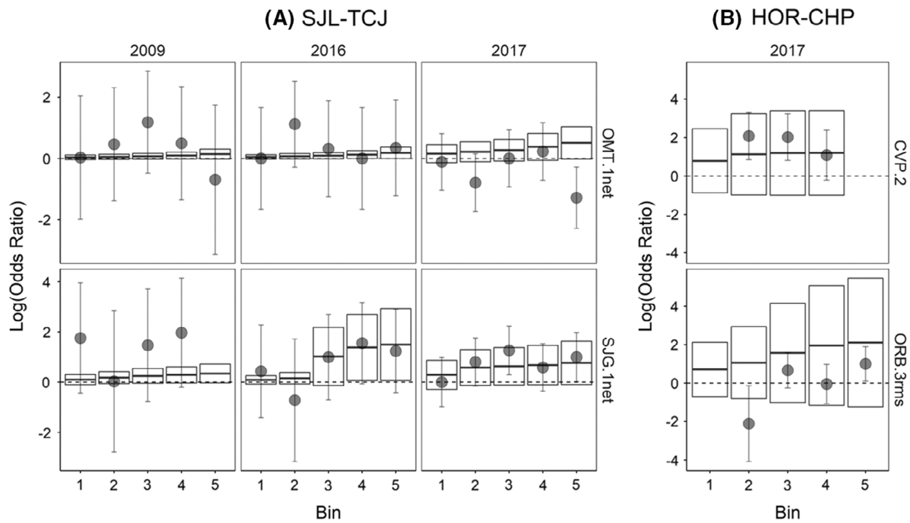

FIGURE 3. Model assessment results for the 2010–2014 model (Buchanan and Skalski 2020) compared to new data from 2009, 2016, and 2017 for **(A)** the San Joaquin River reach from Lathrop (SJL) to the Turner Cut Junction (TCJ) and **(B)** the head of Old River (HOR) to Chipps Island (CHP). Bin number refers to the range of covariate values as shown in Figure 2 (for HOR–CHP) and Supplemental Figure S1 (for SJL–TCJ). Boxes are prediction ranges of the log odds ratio (LOR) from the 2010–2014 model comparing the binned covariate to the reference bin (bin 0 in Figure 2 and Supplemental Figure S1; central horizontal bar = point estimate; upper and lower boundaries = upper and lower 95% confidence limits). Filled circles are point estimates of LORs from the new year, comparing the bin to the reference bin; error bars are asymptotic 95% confidence intervals. Consistent model predictions are indicated when the filled circles fall inside the prediction boxes.

TABLE 6. Single-variable regression results for survival from the SJL/ORE telemetry stations (codes are defined in Table 3) at the head of Old River (HOR) to Chipps Island (CHP station), adjusted for fixed water year effects, migration route selection at the HOR, the physical barrier at the HOR, and FL at tagging, 2010–2017. See Table 4 for definition of covariates. Sign refers to the estimated regression coefficient (P = P-value from F-test [df = 1, 105]; ΔAIC = difference in Akaike's information criterion; AUC = area under the curve for the receiver operating characteristic curve).

Name	Type	Sign	P	ΔAIC	AUC
ORB.3rms	Flow	+	0.046	0.00	0.78
OMT.3rms	Flow	+	0.064	4.76	0.77
CVP.2	Exports	+	0.095	10.56	0.76
VNS.2	Delta inflow ($\log_e$ scale)	+	0.124	14.33	0.76
SWP.2	Exports	+	0.312	26.62	0.74
IE.2	Inflow: export ratio ($\log_e$ scale)	–	0.475	31.32	0.72
MID.3net	Flow	–	0.535	32.47	0.72
OMT.3net	Flow	–	0.543	32.60	0.72
Tslt.2	Temperature	–	0.817	35.54	0.73

= 59) resulted in low statistical power and a relatively high P-value ($P = 0.09$) compared to the full-data model ($P = 0.046$). The moderately weak support for an association between survival and the CVP export rate observed using the full data ($P = 0.095$) was notably poorer without the 2011 data ($P = 0.54$).

The migration routing assessment found small differences in predicted survival to Chipps Island depending on WY type and covariate values, but there was high uncertainty in the model predictions (Figure 4). For the dry WYs, the SJR route (i.e., the physical barrier at the HOR was present) was predicted to have slightly higher survival than the OR route (i.e., barrier absent) for Delta inflow (VNS.2) greater than approximately 85 m^3/s, although with very high uncertainty (Figure 4C). This contrasts with the normal and wet WYs (barrier absent), for which survival was predicted to be higher in the OR route, especially for CVP exports greater than approximately 71 m^3/s and for a volume (i.e., RMS) of ORB flow greater than approximately 255 m^3/s (Figure 4D–I). Neither CVP exports nor volume of ORB flow was determined to affect route-specific survival in dry years, largely because survival predictions were extraordinarily low under those conditions.

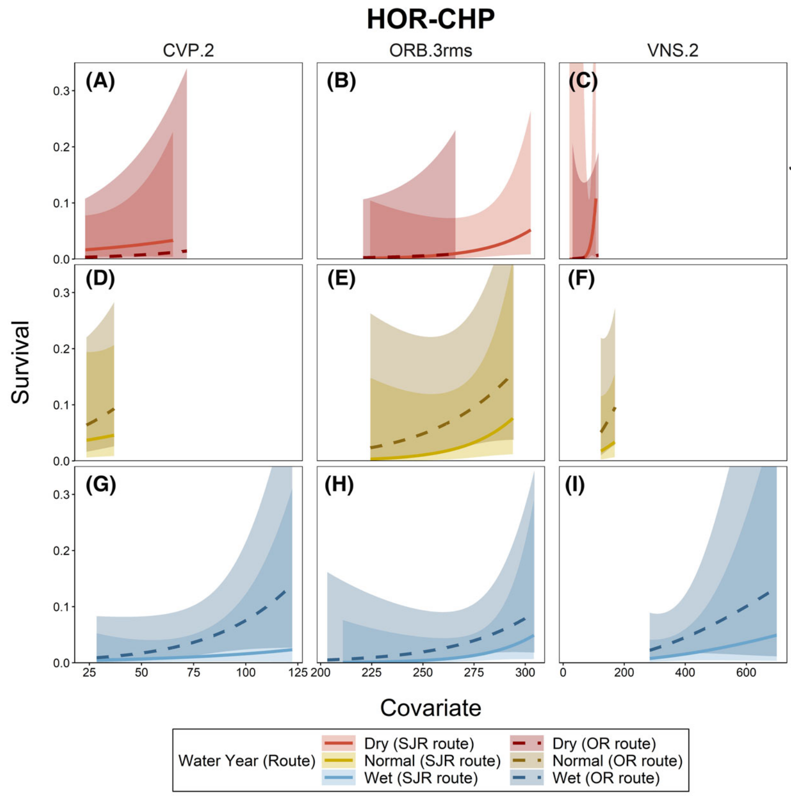

FIGURE 4. Predicted survival and 95% confidence interval band for survival from the head of Old River (HOR; i.e., the SJL and ORE telemetry stations; codes are defined in Table 3) to Chipps Island (CHP station) as a function of the 2-d average Central Valley Project export rate (CVP.2), the 3-d root mean square of Old River (OR) flow at Bacon Island (ORB.3rms), and the 2-d average Delta inflow measured at the VNS station (VNS.2). Solid lines represent the modeled relationship for the San Joaquin River (SJR) route from the HOR, and dashed lines represent the relationship for the OR route. Survival predictions for the dry water year type are shown with the physical barrier in place for the SJR route and without the physical barrier for the OR route. Survival was predicted for fish of average FL at tagging (107 mm).

Lathrop to Turner Cut Junction.— Estimated detection probabilities at the MAC and TRN telemetry stations were consistently 0.97 or greater (Supplemental Table S1), indicating little if any limitation to drawing inferences to survival from the known-fate model. There was strong support for associations between survival to the TCJ and water temperature, Delta inflow, the I:E ratio, and OMT flow ($P < 0.001$); the water temperature model (Tslt.2) had the highest AIC rank (AIC difference [ΔAIC] $\geq$ 41.89; Table 7). The SJR flow at SJG was also associated with survival ($P = 0.002$), but all observations for the 2014 study year were missing. Survival to the TCJ was consistently very low in the single dry WY, during which there was no physical barrier at the HOR (2013; Figure 5A, B). Survival was negatively associated with temperature and positively associated with Delta inflow for dry years when the barrier was installed and also for normal and wet years (barrier absent; Figure 5A, B). All models considered had acceptable AUC values (AUC = 0.70–0.74). Similar results were found when the models were refit without the 2011 study year, except for a lack of support for survival relationships with either interior Delta flow at OMT or the combined export rate ($P \geq 0.22$).

Head of Old River to facilities and Highway 4.— The estimated conditional detection probabilities at the FH4 telemetry stations (CVP, CCF, OR4, and MR4) were at least 0.95 (Supplemental Table S1). Water temperature and Delta inflow again defined the top-ranked models for survival to the FH4 region ($P = 0.01$ for Tslt.2, $P = 0.02$ for VNS.2; Figure 5C, D), although no model had an AUC above 0.68 (Table 8). Survival in this region was estimated to be higher during periods of lower water temperatures and higher Delta inflow conditions. Although steeper slopes were estimated for the dry WYs when the physical barrier was installed, the low sample sizes when the barrier was in place resulted in high uncertainty about the relationships with the barrier (Figure 5C, D). Only the water temperature model ($P = 0.02$) accounted for significant variance in survival in this region when the 2011 data were omitted ($P \geq 0.12$ for all other covariates).

TABLE 7. Single-variable regression results for the joint probability of survival from the San Joaquin River near Lathrop (SJL station) to the Turner Cut Junction (TCJ) and detection at the MAC or TRN station (SJL–TCJ; codes are defined in Table 3), adjusted for fixed water year effects, the physical barrier at the head of Old River, and FL at tagging, 2009–2017. See Table 4 for definition of covariates. Sign refers to the estimated regression coefficient (P = P-value from F-test [df = 1, 783]; ΔAIC = difference in Akaike's information criterion; AUC = area under the curve for the receiver operating characteristic curve).

Name	Type	Sign	P	ΔAIC	AUC
Tslt.2	Temperature	−	<0.001	0.00	0.74
VNS.2	Delta inflow ($\log_e$ scale)	+	<0.001	41.89	0.72
IE.2	Inflow : export ratio ($\log_e$ scale)	+	<0.001	52.49	0.73
OMT.1net	Flow	+	<0.001	61.50	0.73
SJG.1net[a]	Flow	+	0.002	NA	0.70
CVPSWP.2	Exports	−	0.045	98.61	0.72

[a]SJG.1net observations were missing for all records from 2014. The F-test is based on df = 1, 780.

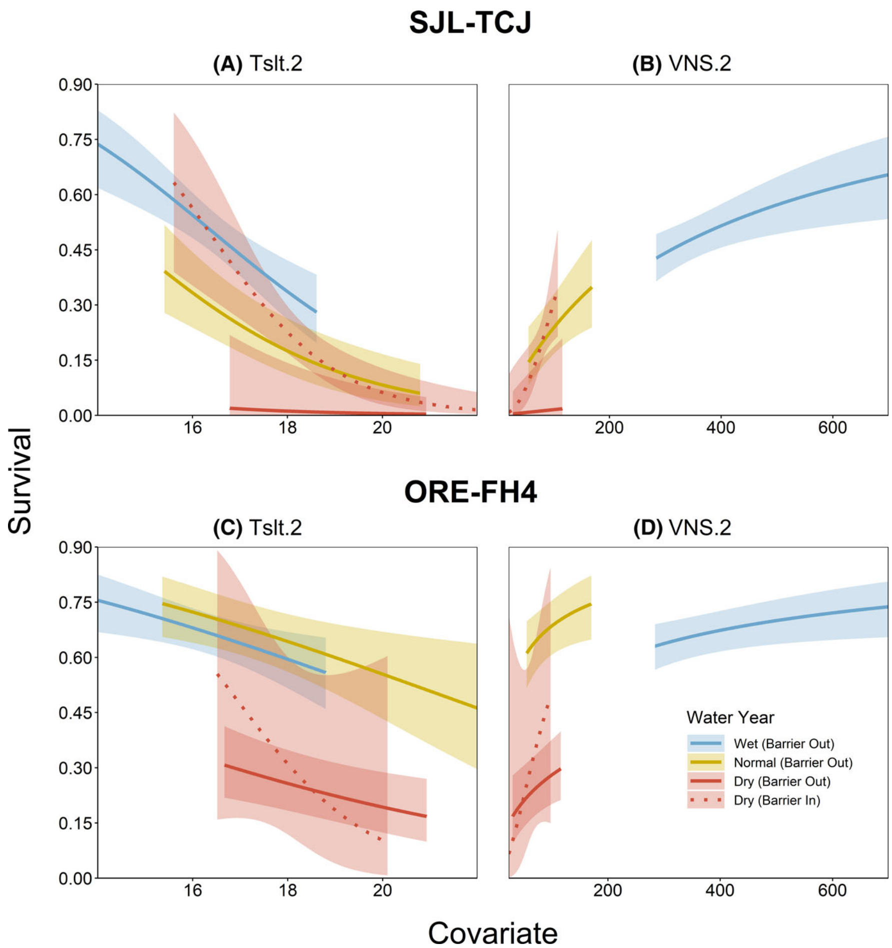

FIGURE 5. Predicted survival and 95% confidence interval band for survival **(A)**, **(B)** from the San Joaquin River near Lathrop (SJL) to the Turner Cut Junction (TCJ; MAC and TRN telemetry stations; codes are defined in Table 3) and **(C)**, **(D)** from Old River (OR) near its head (ORE station) to the FH4 region (CVP, CCF, OR4, and MR4 stations) as a function of San Joaquin River water temperature at the SLT station (Tslt.2) and Delta inflow measured at the VNS station (VNS.2). Dotted lines represent the modeled relationship when the physical barrier was installed at the head of OR, and solid lines represent the modeled relationship when the physical barrier was absent. Survival was predicted for fish of average FL at tagging (107 mm).

DISCUSSION

Chinook Salmon have been in decline across many portions of their western North American range over the past decades (Welch et al. 2021). High ocean mortality and climate change have made boosting survival through the freshwater and estuarine life stages all the more important

TABLE 8. Single-variable regression results for the joint probability of survival from the ORE telemetry station to the water export facilities/Highway 4 (FH4) region of the interior Delta and detection at the CVP, CCF, OR4, or MR4 (ORE–FH4; codes are defined in Table 3) telemetry station, adjusted for fixed water year effects, the physical barrier at the head of Old River, and FL at tagging, 2009–2017. See Table 4 for definition of covariates. Sign refers to the estimated regression coefficient (P = P-value from F-test [df = 1, 570]; ΔAIC = difference in Akaike's information criterion; AUC = area under the curve for the receiver operating characteristic curve).

Name	Type	Sign	P	ΔAIC	AUC
Tslt.2	Temperature	–	0.014	0.00	0.67
VNS.2	Delta inflow ($\log_e$ scale)	+	0.022	2.89	0.68
OMT.1net	Flow	+	0.157	15.29	0.67
OMT.1rms	Flow	+	0.158	15.35	0.67
IE.2	Inflow : export ratio ($\log_e$ scale)	+	0.173	15.86	0.67
CVPSWP.2	Exports	+	0.824	22.85	0.66

to population persistence (Crozier et al. 2021). However, studying estuarine life stages and identifying their survival patterns can be challenging (Buchanan et al. 2021). Opportunities to reevaluate previous findings with new data are rare in ecology, where data collection is arduous and studies are expensive, but they are vital to scientific learning and effective management. Here, the availability of new telemetry data allowed us to assess previous findings and update thinking on the prevailing conceptual model.

An understanding of the effects of water management actions on survival patterns of emigrating juvenile Chinook Salmon in the Delta has evolved with the collection of acoustic telemetry data in recent years. Earlier understanding was based largely on coded wire tag data and adult escapement data for both SR and SJR stocks, and through-Delta survival was predicted to be higher for greater inflow, lower water exports, and greater use of main-stem routes (Newman 2003; Newman and Brandes 2010; SST 2017). Some of these predictions have been maintained with acoustic telemetry data for SR stocks but are equivocal for SJR salmon. Telemetry studies have confirmed the importance of route selection and, to a lesser extent, the effect of Delta inflow for SR stocks (Perry et al. 2010, 2018; Singer et al. 2013; Michel et al. 2015). In contrast, Buchanan et al. (2013, 2018) observed that Delta survival of SJR salmon was low in wet years as well as dry years and that the interior Delta route often had survival equal to or slightly higher than that in the main-stem route. Furthermore, the salvage (exports) route may be relevant to successful Delta emigration for southern Delta salmon despite considerable mortality risks at the facilities (Buchanan et al. 2018). These results were confirmed by Buchanan and Skalski (2020), who additionally found evidence that survival to Chipps Island was related to mid-Delta flow but not to the barrier at the HOR. However, route selection at the TCJ appears to be more important, with especially low survival for Turner Cut fish, demonstrating regional differences in mortality risk within the interior Delta (SST 2017). A similar route effect was observed at Turner Cut for steelhead (Buchanan et al. 2021).

The relationship between Delta inflow and salmon survival is of paramount importance because of reductions in spring inflow resulting from upstream dam operations and increases in drought conditions expected in the coming decades (Diffenbaugh et al. 2015). Erkkila et al. (1950) observed very low juvenile survival of SJR salmonids in a drought year before modern water pumping operations began. This observation provides precedent to the very low survival observed in the 2012–2015 acoustic telemetry data and supports the idea of inflow as a determinant of survival. However, very low survival was also observed in the wet years of 2011 and 2017. Both this study and the Buchanan and Skalski (2020) study found a positive relationship between Delta inflow and survival in the upper reaches of the SJR route through the Delta, and the present study found a similar pattern for the upper reaches of the OR route, but the estimated effect on the scale of the entire Delta was small and highly uncertain (Figure 4). A similarly localized effect of inflow has been observed for late-fall-run Chinook Salmon in the SR (Perry et al. 2018) and steelhead in the SJR (Buchanan et al. 2021). The inflow effect appears to cease where the habitat changes from predominantly riverine to predominantly tidal (Perry et al. 2018).

Although we expected lower survival out of the Delta when exports were higher, the 2010–2017 acoustic telemetry data provided no evidence of that. Instead, the data were more consistent with a positive association between CVP exports and survival, especially in the OR route during wet years (Figure 4), although these findings were accompanied by considerable uncertainty and depended on a single study year (2011). A stronger export effect in the OR route is consistent with hydrodynamic modeling and coded wire tag studies that show larger effects of export rates in regions closer to or directly connected to the export facilities (Zeug and Cavallo 2014; Cavallo et al. 2015). Increased export rates are expected to draw migrating salmon from the HOR to the facilities; thus, we expected a positive effect of combined exports on survival to the FH4 region. However, no such relationship was observed (Table 8). We explored further by refitting the OR model using only detections at the CVP as the response variable and we found moderate support for a positive relationship between transition to the CVP and combined exports (CVP + SWP; $P = 0.03$), but model fit was poor (AUC = 0.62). We note that these data were collected under a policy of export restrictions designed to protect migrating salmonids and other native fishes (NMFS 2009); therefore, this analysis was a test of opportunistic, short-term manipulation of exports allowed within that policy rather than a test of the entire impact of over 80 years of export operations.

The barrier at the HOR was intended to limit fish entry into OR and entrainment at the facilities. These data show no obvious survival benefit to remaining in the SJR, and the barrier has not been installed in recent years. Without the barrier, the majority of smolts are expected to enter OR, especially under high flows (Cavallo et al. 2015) or high exports (Cavallo et al. 2013). This is expected to result in more fish salvaged and transported by truck out of the Delta but also to result in higher loss within and near the facilities. Furthermore, Buchanan et al. (2021) found a larger benefit of Delta inflow on steelhead survival in the SJR route when the barrier was in place; a similar pattern was observed in this study for dry years, although the predicted responses had high uncertainty, especially on the through-Delta scale (Figures 4, 5B). This pattern may be due to increased flows in the SJR between the HOR and Turner Cut when the barrier is in place, which may help juvenile salmon to evade predation by increasing turbidity, decreasing temperature, improving other components of water quality, and delaying entry into brackish water (Sinokrot and Gulliver 2000; Monsen et al. 2007; Lehman et al. 2017; Hause 2020). Without the barrier in place, water quality in the SJR upstream of Turner Cut may be severely degraded when Delta inflows are low (Monsen et al. 2007), contributing to the low survival observed to the TCJ, especially in low-flow years.

Both the original modeling exercise in Buchanan and Skalski (2020) and this updated analysis found an association between interior Delta flow conditions and survival in the Delta, although not the one suggested by the conceptual model (Table 1). A positive relationship was expected between average net interior Delta flows and survival to Chipps Island based on the idea that more positive flow in the western interior Delta region would help fish to avoid delay or loss at the water export facilities. This idea is the basis of management strategies that limit negative flows in the interior Delta when juvenile salmonids are present. Those strategies are most obviously targeted at salmonids that enter the Delta from the north (e.g., from the SR), that can avoid the southern Delta entirely and may be deterred from approaching the FH4 region by limiting negative flows, and for which an increased mortality risk of entering the interior Delta has been observed (Perry et al. 2010; Singer et al. 2013). The potential benefit of these strategies to SJR basin salmonids is more complex, reflecting both the arrival of these fish in the western OR region coming from the south and the multiple exit routes from this region (past Highway 4 versus the facilities), and this complexity was demonstrated by the lack of an association between directed OMT flows (OMT.1net and OMT.3net) and survival either to the FH4 region (Table 8) or overall to Chipps Island (Table 6). When the response variable was restricted to detection at the CVP, a negative relationship was observed with OMT.1net ($P = 0.06$); this is consistent with predictions, although support was moderate and model fit was poor (AUC = 0.61). Additionally, inference in this case is to a combination of survival and selecting the CVP route rather than to survival alone.

Instead of the net flow, it was the RMS of OR flow in the interior Delta that was most related to survival to Chipps Island, with a greater volume of water movement at Bacon Island (ORB) being associated with higher survival. This pattern was observed in both the original 2010–2014 model and the updated analysis and for both the OR and SJR routes, although there remains considerable uncertainty about model predictions (Figure 4). No relationship was observed between the RMS of OR/MR flow and survival in the upper reaches of either the OR route (Table 8) or the SJR route (results not shown), suggesting that this measure is indicative of habitat conditions in the downstream reaches of the Delta. Hydrodynamics in these regions are most affected by tidal fluctuations, exports, and SR inflow to the Delta; little SJR water reaches these regions, especially under conditions of low inflow or high exports (Monsen et al. 2007; Cavallo et al. 2013). The RMS measure reflects the volume of water movement rather than its direction, and different sources may contribute to it at different phases of the tidal cycle. Overall, spring tides may produce higher RMS values than neap tides because of the larger tidal fluctuations. Within each subdiurnal tidal cycle, export operations may contribute more to RMS on flood tides when the CCF gates open to draw water off OR, whereas Delta inflow (mostly from the SR) may contribute more on ebb tides. The lack of support for the net flow metrics for survival to Chipps Island suggests that the potential routing effect of interior Delta flow patterns is not driving survival patterns in this region—rather, the physical and biological effects of having more water present promote survival.

Two ideas that have received more attention in recent years are spatial heterogeneity in survival processes throughout the southern Delta and the role of predation in survival. In this analysis, water temperature and Delta inflow defined the top-ranked models in the upstream reaches but were not highly ranked for the full Delta region. Local habitat conditions in the downstream reaches of the SJR or the interior Delta north of the Highway 4 sites may be associated with survival in those regions. In addition to regional differences in water quality (Hause 2020) and facility entrainment risk, the predator community varies both spatially and temporally (Cutter et al. 2017), resulting in regional differences in the conditions or smolt behaviors that are most conducive to survival. Predatory fish are known to reside in or near the water export facilities, and predation loss within the facilities but before salvage is considered a major component of the direct mortality on the salmon population and other native fishes at the facilities. However, a dense predator community is also apparent in the SJR, associated with patches of submerged aquatic vegetation, littoral habitat, and deep pools (Conrad et al. 2016; Cutter et al. 2017; Loomis 2019; Michel et al. 2020). Focus has historically been on the Striped Bass *Morone saxatilis* as the primary predator of juvenile salmon, but gut evaluation studies of predatory fish between the HOR and Stockton have found that the White Catfish *Ameiurus catus* may also be an important predator in that region (Michel et al. 2018). Largemouth Bass comprise the dominant fish species in some parts of the interior Delta (Young et al. 2018). The benefit of increased inflow between the HOR and Turner Cut and of increased water movement in the downstream Delta reaches may stem partly from lower temperatures, increased turbidity, and improved protection from visual predators (Ferrari et al. 2014; Michel et al. 2020). Daily or subdaily characterizations of predation activity by piscivorous fishes and avian species may help to resolve some of the uncertainty seen in current model predictions (Michel et al. 2020). Other potential variables to consider are measures of fish health, physical habitat, and water quality (Evans et al. 2014; Lehman et al. 2017, 2020; Moyle et al. 2017; Hause 2020). However, sparse detection data in the downstream reaches have limited the ability to characterize survival processes in those regions, and additional tagging studies targeting the lower SJR and northern interior Delta regions are recommended.

A key benefit to collecting more data for this system was the opportunity to develop new models based on WY type rather than calendar year. Surface water management in California uses the WY type framework to inform water export operations each year, so results using WY type are anticipated to be useful as management tools. The new models here provide predictions for three categories of WY: wet, normal, and dry, where "normal" and "dry" each combine two of the five hydrological management WY types defined by CDWR (Table 2). Although considerably more useful to managers than the original calendar year models, these WY models still depend on only a few years representing any single WY type. Furthermore, they fail to capture some hydrological-based variability because they required pooling adjacent CDWR WY definitions to accommodate a data set of only 8 years. We recommend further development of the WY models should additional data become available.

An additional benefit of having new data was assessment of the previous (2010–2014) model and the insight provided by such assessment. Comparing predictions from the original model to the out-of-sample data was complicated by the fixed year effects of the 2010–2014 model (Buchanan and Skalski 2020) and required indirect assessment via relative comparisons using LORs. Assessment was further hampered by the low levels of Delta survival in even the top-performing years and the nonuniform distributions of observed covariates in the new study years. Nevertheless, the model assessment demonstrated moderate to good fit of the 2010–2014 models to the 2017 data for both the HOR–CHP and SJL–TCJ reaches and poorer fit to the 2009 and 2016 data. 2017 was a wet year, and 2009 and 2016 were below-normal and dry years, respectively. Thus, the original HOR–CHP and SJL–TCJ models may be considered "wet year" models, even though they were based on studies from multiple years representing four WY types. Collection of additional data with sufficient sample sizes under dry and drought conditions will be necessary to provide full guidance to managers seeking to maintain salmon populations under the more frequent and extreme drought conditions expected under climate change (Diffenbaugh et al. 2015).

Although only 1 of the 5 years of data used in the original analysis was a wet year (2011), that year accounted for the majority (52%) of the data available for the 2010–2014 model. The dependence of the original modeling results on the 2011 study year was an important but unobservable question without additional data. The new models using data from the years 2009–2017 were again based on a plurality of wet year records (47%), but the availability of a second wet year (2017) facilitated distinguishing between year and hydrologic effects. In most cases, the 2009–2017 models provided similar results with and without the 2011 data. The biggest exception was the reduction in support for the interior Delta (OMT) flow model for the predominantly riverine reach between SJL and TCJ when 2011 data were excluded. The sensitivity of this (unexpected) result to a single year's data underscores the importance of replicating results in scientific investigations—especially results without a clear mechanistic relationship and those based on only a few study years, an unbalanced study design, or observational studies.

Even with the additional data and updated findings, there remain some limitations in the ability to apply these results directly to the fall-run Chinook Salmon population at large. The existing data reflect salmon that migrate through the Delta as subyearling smolts in the spring; thus, they miss any salmon that enter the Delta earlier in the year as fry. Furthermore, these data represent hatchery fish, which are known to have different survival propensities than wild fish (Evans et al. 2014). Acquiring a sufficient number of naturally spawned salmon to tag may be impractical, but it may instead be possible in future studies to investigate known or proposed differences between hatchery and wild populations. For example, infections among hatchery fish have been observed at high rates (Naish et al. 2007) and are exacerbated at the higher temperatures that are prevalent under dry and drought conditions. Understanding the role of disease in the survival of hatchery fish and the rate of such diseases in the wild population will help to relate survival results from studies of hatchery fish to the wild population (Lehman et al. 2020).

This work has several management implications. In the absence of a single factor that accounts for a high amount of survival variability throughout all regions of the Delta, it will be necessary to combine multiple strategies to improve salmon survival in this region. Increases in inflow are predicted to improve salmon survival through the upper reaches of the Delta, especially in dry years when a physical barrier is in place at the HOR. Merely releasing water from upstream without also installing the barrier will not realize the full potential of the reservoir releases. Thus, managers should reconsider the decision not to install the barrier during dry years. In the absence of the barrier, the CVP salvage route will become more important and managers should work to improve facility and salvage survival. High flows should be promoted in regions north of Highway 4 and Turner Cut by allowing SR water to enter the interior Delta rather than proposed diversion of this water around the Delta to the export facilities. However, dependence on manipulations of Delta inflow and export rates is unlikely to produce survival that would be high enough to stabilize the population. Instead, we recommend that managers also address habitat conditions that have resulted from decades of reduced inflow and water extraction, including low turbidity and dissolved oxygen, high water temperatures, and littoral patches of submerged aquatic vegetation that provide cover for predators, such as juvenile Largemouth Bass. Consistent removal of submerged aquatic vegetation in the most commonly used routes may boost salmon survival opportunities (Loomis 2019), especially if combined with installation of the OR barrier and reservoir releases that are timed to the peak of the salmon emigration.

The Central Valley fall-run Chinook Salmon population is not currently listed as a protected species under the Endangered Species Act. However, juvenile emigration survival through the Delta has been markedly low for more than a decade, and more frequent, intense, and prolonged drought events from a warming climate will place this population in increased jeopardy. The persistence of this population will require effective management of water resources, land use practices, hatcheries, and fish populations. Identifying effective strategies will require ongoing population monitoring, retesting old predictions against new data, and updating existing models. The process of continued data collection and independent validation is both important and humbling work. It is an opportunity to refine explanatory variables, hone hypotheses that can withstand the test of further scrutiny, and develop the basis of mechanistic models that promote understanding of the system as a whole. Such work also requires reckoning with past misapprehensions—a sometimes uncomfortable but always valuable exercise. These key elements to science-based management will be especially important for preserving imperiled populations and ensuring effective resource management as the climate warms and as the habitat and ecosystem change.

ACKNOWLEDGMENTS

Many individuals from several agencies made this project possible. The 2009 and 2010 studies and the first two release groups from 2011 were part of the Vernalis Adaptive Management Program (VAMP) study, and the last two groups from 2011 were part of the South Delta Temporary Barriers study funded by CDWR (SJRGA 2011, 2013). The VAMP study was funded by the San Joaquin River Group Authority. The 2012–2017 studies were part of the south Delta Chinook Salmon survival study; they were conducted jointly by the U.S. Fish and Wildlife Service (USFWS), U.S. Bureau of Reclamation (USBR), USGS, and University of Washington and were funded by the Central Valley Project Improvement Act's (CVPIA) Comprehensive Monitoring and Assessment Program, CDWR, and USBR. Funds for this analysis and manuscript preparation were provided by the USFWS through the CVPIA. We are grateful to the many people and agencies who funded, oversaw, and implemented fish tagging, care, and release as well as acoustic receiver installation, maintenance, retrieval, and processing. We thank Chris Holbrook (USGS) for primary analysis of the 2016 and 2017 data, and we appreciate the two anonymous reviewers for their helpful suggestions on the manuscript. There is no conflict of interest declared in this article.

REFERENCES

Arthur, J. F., M. D. Ball, and S. Y. Baughman. 1996. Summary of federal and state water project environmental impacts in the San Francisco Bay–Delta estuary, California. Pages 445–495 *in* J. T. Hollibaugh, editor. San Francisco Bay: the ecosystem: further investigations into the natural history of San Francisco Bay and Delta with reference to the influence of man. San Francisco State University, San Francisco, California.

Barnard, D., P. Brandes, D. LaPlante, K. Nichols, and R. Buchanan. 2022. 2016 south Delta Chinook Salmon survival study: draft report. U.S. Fish and Wildlife Service, Lodi, California.

Bowen, M. D., and R. Bark. 2012. 2010 effectiveness of a non-physical fish barrier at the divergence of the Old and San Joaquin rivers (CA). U.S. Bureau of Reclamation, Technical Service Center, Technical Memorandum 86-68290-10-07, Denver.

Buchanan, R. A., P. L. Brandes, J. Ingram, M. Marshall, K. Nichols, D. LaPlante, D. Barnard, K. Towne, and J. Israel. 2018. 2014 south Delta Chinook Salmon survival study. U.S. Fish and Wildlife Service, Lodi, California.

Buchanan, R. A., P. L. Brandes, M. Marshall, J. S. Foott, J. Ingram, D. LaPlante, and J. Israel. 2015. 2012 south Delta Chinook Salmon survival study. U.S. Fish and Wildlife Service, Lodi, California.

Buchanan, R. A., P. L. Brandes, M. Marshall, K. Nichols, J. Ingram, D. LaPlante, and J. Israel. 2016. 2013 south Delta Chinook Salmon survival study. U.S. Fish and Wildlife Service, Lodi, California.

Buchanan, R. A., P. L. Brandes, and J. R. Skalski. 2018. Survival of juvenile fall-run Chinook Salmon through the San Joaquin River Delta, California, 2010–2015. North American Journal of Fisheries Management 38:663–679.

Buchanan, R. A., E. Buttermore, and J. Israel. 2021. Outmigration survival of a threatened steelhead population through a tidal estuary. Canadian Journal of Fisheries and Aquatic Sciences 78:1869–1886.

Buchanan, R. A., and J. R. Skalski. 2020. Relating survival of fall-run Chinook Salmon through the San Joaquin Delta to river flow. Environmental Biology of Fishes 103:389–410.

Buchanan, R. A., J. R. Skalski, P. L. Brandes, and A. Fuller. 2013. Route use and survival of juvenile Chinook Salmon through the San Joaquin River Delta. North American Journal of Fisheries Management 33:216–229.

Buchanan, R. A., and S. L. Whitlock. 2022. Diagnosing predated tags in telemetry survival studies of migratory fishes in river systems. Animal Biotelemetry 10:article 13.

Burnham, K. P., and D. R. Anderson. 2002. Model selection and multimodel inference: a practical information-theoretic approach, 2nd edition. Springer, New York.

Cavallo, B., P. Gaskill, and J. Melgo. 2013. Investigating the influence of tides, inflow, and exports on sub-daily flow in the Sacramento–San Joaquin Delta. Cramer Fish Sciences, Auburn, California.

Cavallo, B., P. Gaskill, J. Melgo, and S. C. Zeug. 2015. Predicting juvenile Chinook Salmon routing in riverine and tidal channels of a freshwater estuary. Environmental Biology of Fishes 98:1571–1582.

Conrad, J. L., A. J. Bibian, K. L. Weinersmith, D. De Carion, M. J. Young, P. Crain, E. L. Hestir, M. J. Santos, and A. Sih. 2016. Novel species interaction in a highly modified estuary: association of Largemouth Bass with Brazilian waterweed *Egeria densa*. Transactions of the American Fisheries Society 145:249–263.

Conroy, M. J., and J. T. Peterson. 2013. Decision making in natural resource management: a structured, adaptive approach. Wiley, Hoboken, New Jersey.

Crozier, L. G., B. J. Burke, B. E. Chasco, D. L. Widener, and R. W. Zabel. 2021. Climate change threatens Chinook Salmon throughout their life cycle. Communications Biology 4:article 222.

Cutter, G. R. Jr., S. C. Manugian, J. Renfree, J. Smith, C. Michel, D. Huff, T. S. Sessions, B. E. Elliot, K. Stierhoff, S. Mau, D. Murfin, and D. A. Demer. 2017. Mobile acoustic sampling to map bathymetry and quantify the densities and distributions of salmonid smolt predators in the San Joaquin River. NOAA Technical Memorandum NMFS-SWFSC-575.

Diffenbaugh, N. S., D. L. Swain, and D. Touma. 2015. Anthropogenic warming has increased drought risk in California. Proceedings of the National Academy of Sciences of the United States of America 112:3931–3936.

Duncan, J. R., and J. L. Lockwood. 2001. Extinction in a field of bullets: a search for causes in the decline of the world's freshwater fishes. Biological Conservation 102:97–105.

Erkkila, L. F., J. W. Moffett, O. B. Cope, B. R. Smith, and R. S. Nielson. 1950. Sacramento–San Joaquin Delta fishery resources: effects of Tracy Pumping Plant and Delta Cross Channel. U.S. Fish and Wildlife Service Special Scientific Report Fisheries 56.

Evans, A. F., N. J. Hostetter, K. Collis, D. D. Roby, and F. J. Loge. 2014. Relationship between juvenile fish condition and survival to adulthood in steelhead. Transactions of the American Fisheries Society 143:899–909.

Ferrari, M. C. O., L. Ranåker, K. L. Weinersmith, M. J. Young, A. Sih, and J. L. Conrad. 2014. Effects of turbidity and an invasive waterweed on predation by introduced Largemouth Bass. Environmental Biology of Fishes 97:79–90.

Fisher, F. W. 1994. Past and present status of Central Valley Chinook Salmon. Conservation Biology 8:870–873.

Gingras, M. 1997. Mark/recapture experiments at Clifton Court Forebay to estimate pre-screening loss to entrained juvenile fishes: 1976–1993. California Department of Fish and Game, Interagency Ecological Program, Technical Report 55, Sacramento.

Grimaldo, L. F., T. Sommer, N. Van Ark, G. Jones, E. Holland, P. B. Moyle, B. Herbold, and P. Smith. 2011. Factors affecting fish entrainment into massive water diversions in a tidal freshwater estuary: can fish losses be managed? North American Journal of Fisheries Management 29:1253–1270.

Hance, D. J., R. W. Perry, J. M. Plumb, and A. C. Pope. 2020. A temporally stratified extension of space-for-time Cormack–Jolly–Seber for migratory animals. Biometrics 76:900–912.

Hause, C. 2020. Outmigration survival of juvenile spring-run Chinook Salmon in relation to physicochemical conditions in the San Joaquin River. Master's thesis. University of California–Davis, Davis.

Hosmer, D. W., and S. Lemeshow. 2000. Applied logistic regression, 2nd edition. Wiley, New York.

Hurlbert, S. H. 1984. Pseudoreplication and the design of ecological field experiments. Ecological Monographs 54:187–211.

Jassby, A. D., W. J. Kimmerer, S. G. Monismith, C. Armor, J. E. Cloern, T. M. Powell, J. R. Schubel, and T. J. Vendlinski. 1995. Isohaline position as a habitat indicator for estuarine populations. Ecological Applications 5:272–289.

Kehoe, L. J., J. Lund, L. Chalifour, Y. Asadian, E. Balke, S. Boyd, D. Carlson, J. M. Casey, B. Connors, N. Cryer, M. C. Drever, S. Hinch, C. Levings, M. MacDuffee, H. McGregor, J. Richardson, D. C. Scott, D. Stewart, R. G. Vennesland, C. E. Wilkinson, P. Zevit, J. K. Baum, and T. G. Martin. 2021. Conservation in heavily urbanized biodiverse regions requires urgent management action and attention to governance. Conservation Science and Practice 3 (2):e310.

Kimmerer, W. J. 2002. Physical, biological, and management responses to variable freshwater flow into the San Francisco Estuary. Estuaries 25:1275–1290.

Kimmerer, W. J. 2008. Losses of Sacramento River Chinook Salmon and Delta Smelt to entrainment in water diversions in the Sacramento–San Joaquin Delta. San Francisco Estuary and Watershed Journal 6(2):article 2.

Kimmerer, W. J., and M. L. Nobriga. 2008. Investigating particle transport and fate in the Sacramento–San Joaquin Delta using a particle tracking model. San Francisco Estuary and Watershed Journal 6(1): article 4.

Lehman, B., D. D. Huff, S. A. Hayes, and S. T. Lindley. 2017. Relationships between Chinook Salmon swimming performance and water quality in the San Joaquin River, California. Transactions of the American Fisheries Society 146:349–358.

Lehman, B. M., R. C. Johnson, M. Adkison, O. T. Burgess, R. E. Connon, N. A. Fangue, J. S. Foott, S. L. Hallett, B. Martinez-Lopez, K. M. Miller, M. K. Purcell, N. A. Som, P. Valdes Donoso, and A. L. Collins. 2020. Disease in Central Valley salmon: status and lessons from other systems. San Francisco Estuary and Watershed Science 18 (3):article 2.

Loomis, C. M. 2019. Density and distribution of piscivorous fishes in the Sacramento–San Joaquin Delta. Master's thesis. Humboldt State University, Arcata, California.

Michel, C. J., A. J. Ammann, S. J. Lindley, P. T. Sandstrom, E. D. Chapman, M. J. Thomas, G. P. Singer, A. P. Klimley, and R. B. MacFarlane. 2015. Chinook Salmon outmigration survival in wet and dry years in California's Sacramento River. Canadian Journal of Fisheries and Aquatic Sciences 72:1749–1759.

Michel, C. J., M. J. Henderson, C. M. Loomis, J. M. Smith, N. J. Demetras, I. S. Iglesias, B. M. Lehman, and D. D. Huff. 2020. Fish predation on a landscape scale. Ecosphere 11(6):e03168.

Michel, C. J., J. M. Smith, N. J. Demetras, D. D. Huff, and S. A. Hayes. 2018. Non-native fish predator density and molecular-based diet estimates suggest differing effects of predator species on juvenile salmon in the San Joaquin River, California. San Francisco Estuary and Watershed Science 16(4):article 3.

Monsen, N. E., J. E. Cloern, and J. R. Burau. 2007. Effects of flow diversions on water and habitat quality: examples from California's highly manipulated Sacramento–San Joaquin Delta. San Francisco Estuary and Watershed Science 5(3):article 2.

Moyle, P. B., R. A. Lusardi, P. J. Samuel, and J. V. E. Katz. 2017. State of the salmonids: status of California's emblematic fishes 2017. Center for Watershed Sciences, University of California–Davis, Davis, and California Trout, San Francisco.

Naish, K. A., J. E. Taylor III, P. S. Levin, T. P. Quinn, J. R. Winton, D. Huppert, and R. Hilborn. 2007. An evaluation of the effects of conservation and fishery enhancement hatcheries on wild populations of salmon. Advances in Marine Biology 53:61–194.

Nam, B.-H., and R. B. D'Agostino. 2002. Discrimination index, the area under the ROC curve. Pages 267–279 *in* C. Huber-Carol, N. Balakrishnan, M. S. Nikulin, and M. Mesbah, editors. Goodness-of-fit tests and model validity. Birkhäuser, Boston.

Nehlsen, W., J. E. Williams, and J. A. Lichatowich. 1991. Pacific salmon at the crossroads: stocks at risk from California, Oregon, Idaho, and Washington. Fisheries 16(2):4–21.

Newman, K. B. 2003. Modelling paired release–recovery data in the presence of survival and capture heterogeneity with application to marked juvenile salmon. Statistical Modelling 3:157–177.

Newman, K. B., and P. L. Brandes. 2010. Hierarchical modeling of juvenile Chinook Salmon survival as a function of Sacramento–San Joaquin Delta water exports. North American Journal of Fisheries Management 30:157–169.

NMFS (National Marine Fisheries Service). 2009. Endangered Species Act Section 7 consultation: biological opinion and conference opinion on the long-term operations of the Central Valley Project and State Water Project (June 4, 2009; amended April 7, 2011). NMFS, Southwest Region, Long Beach, California.

Perry, R. W., P. L. Brandes, P. T. Sandstrom, A. Ammann, B. MacFarlane, A. P. Klimley, and J. R. Skalski. 2010. Estimating survival and migration route probabilities of juvenile Chinook Salmon in the Sacramento–San Joaquin River Delta. North American Journal of Fisheries Management 30:142–152.

Perry, R. W., A. C. Pope, J. G. Romine, P. L. Brandes, J. R. Burau, A. R. Blake, A. J. Ammann, and C. J. Michel. 2018. Flow-mediated effects on travel time, routing, and survival of juvenile Chinook Salmon in a spatially complex, tidally forced river delta. Canadian Journal of Fisheries and Aquatic Sciences 75:1886–1901.

Poff, N. L., M. M. Brinson, and J. W. Day. 2002. Aquatic ecosystems and global climate change. Pew Center on Global Climate Change, Arlington, Virginia.

R Core Team. 2019. R: a language and environment for statistical computing. R Foundation for Statistical Computing, Vienna.

Reynolds, J. D., T. J. Webb, and L. A. Hawkins. 2005. Life history and ecological correlates of extinction risk in European freshwater fishes. Canadian Journal of Fisheries and Aquatic Sciences 62:854–862.

Sabal, M. C., C. J. Michel, J. M. Smith, A. Hampton, and S. A. Hayes. 2019. Seasonal movement patterns of Striped Bass (*Morone saxatilis*) in their nonnative range. Estuaries and Coasts 42:567–579.

Singer, G. P., A. R. Hearn, E. D. Chapman, M. L. Peterson, P. E. LaCivita, W. N. Brostoff, A. Bremner, and A. P. Klimley. 2013. Interannual variation of reach specific migratory success for Sacramento River hatchery yearling late-fall run Chinook Salmon (*Oncorhynchus tshawytscha*) and steelhead trout (*Oncorhynchus mykiss*). Environmental Biology of Fishes 96:363–379.

Sinokrot, B. A., and J. S. Gulliver. 2000. In-stream flow impact on river water temperatures. Journal of Hydraulic Research 38:339–349.

SJRGA (San Joaquin River Group Authority). 2010. 2009 annual technical report: on implementation and monitoring of the San Joaquin River agreement and the Vernalis Adaptive Management Plan (VAMP). SJRGA, Modesto, California.

SJRGA (San Joaquin River Group Authority). 2011. 2010 annual technical report: on implementation and monitoring of the San Joaquin River agreement and the Vernalis Adaptive Management Plan (VAMP). SJRGA, Modesto, California.

SJRGA (San Joaquin River Group Authority). 2013. 2011 annual technical report: on implementation and monitoring of the San Joaquin River agreement and the Vernalis Adaptive Management Plan (VAMP). SJRGA, Modesto, California.

Skalski, J. R., S. G. Smith, R. N. Iwamoto, J. G. Williams, and A. Hoffmann. 1998. Use of passive integrated transponder tags to estimate survival of migrant juvenile salmonids in the Snake and Columbia rivers. Canadian Journal of Fisheries and Aquatic Sciences 55:1484–1493.

SST (Salmonid Scoping Team). 2017. Effects of water project operations on juvenile salmonid migration and survival in the south Delta. Appendix E: effects of migration behavior and project facilities on juvenile salmonid survival. SST, Sacramento, California.

Towne, K., P. Brandes, K. Nichols, R. Buchanan, A. Ammann, G. Singer, and E. Chapman. 2022. 2017 south Delta Chinook Salmon survival study: draft report. U.S. Fish and Wildlife Service, Lodi, California.

Walters, C. J. 1986. Adaptive management of renewable resources. Macmillan, New York.

Welch, D. W., A. D. Porter, and E. L. Rechisky. 2021. A synthesis of the coast-wide decline in survival of West Coast Chinook Salmon (*Oncorhynchus tshawytscha*, Salmonidae). Fish and Fisheries 22:194–211.

Wenger, S. J., and J. D. Olden. 2012. Assessing transferability of ecological models: an underappreciated aspect of statistical validation. Methods in Ecology and Evolution 3:260–267.

Yoshiyama, R. M., F. W. Fisher, and P. B. Moyle. 1998. Historical abundance and decline of Chinook Salmon in the Central Valley region of California. North American Journal of Fisheries Management 18:487–521.

Young, M. J., F. V. Feyrer, D. D. Colombano, J. L. Conrad, and A. Sih. 2018. Fish–habitat relationships along the estuarine gradient of the Sacramento–San Joaquin Delta, California: implications for habitat restoration. Estuaries and Coasts 41:2389–2409.

Zeug, S. C., and B. J. Cavallo. 2014. Controls on the entrainment of juvenile Chinook Salmon (*Oncorhynchus tshawytscha*) into large water diversions and estimates of population-level loss. PLoS (Public Library of Science) ONE 9(7):e101479.

SUPPORTING INFORMATION

Additional supplemental material may be found online in the Supporting Information section at the end of the article.